STRUCTURE OF THE SOLAR CORONA[1]

By Gordon Newkirk, Jr.
High Altitude Observatory, Boulder, Colorado

Introduction

Recent years have seen varied and intense investigations of the solar corona. To a large extent these have been the result of techniques for observing the corona in ways which, only a short time ago, were unimagined or impractical. Radio telescopes have not only supplemented the more classical optical observations but have revealed the unsuspected existence of transient bursts of particles and magnetohydrodynamic waves. Radar probing of the corona allows direct measurement of the inner solar wind. X-ray and ultraviolet photographs taken above the Earth's atmosphere show the inner corona over the entire solar disk while space-probes outside the magnetosphere measure the density, velocity, and magnetic fields of the outermost regions. Balloon- and satellite-borne coronagraphs promise to yield the long-sought synoptic observation of the intermediate corona. Theoretical studies have described the general character of the solar wind and in doing so have uncovered such intriguing problems as the interaction of the wind with the magnetic field of the Sun. Along with these impressive advances other rather old problems remain as perplexing as ever, for example, the connection of structural features in the intermediate corona with surface features and geomagnetic activity as well as the mechanism of heating the corona. Although the long-unresolved question of the ionization of the corona appears to have been settled, the anomalously high abundance of the iron group of elements in the corona remains unexplained.

These many aspects are not to be reviewed in a single article. Discussions of the heating of the corona and the chromosphere-corona interface as well as the interplanetary plasma and high-energy particles from the Sun appear in other papers in this volume. Likewise, an examination of the local physics of the coronal gas is not included. Our concern will be with the density, temperature, and velocity structure of the corona considered from a phenomenological viewpoint. Even within the restricted scope our treatment may not be exhaustive but, we hope, will illuminate existing problems and areas of future advance.

Overall Density Structure

With the recent addition of space-probe and radio-star occultation measurements, coronal densities are now known from the interface with the chromosphere out to the orbit of Earth (Figure 1 and Table I). Since the merit of various theoretical models of the corona is often judged on their ability to predict the decrease of density with increasing distance from the

[1] The survey of literature for this review was concluded in November 1966.

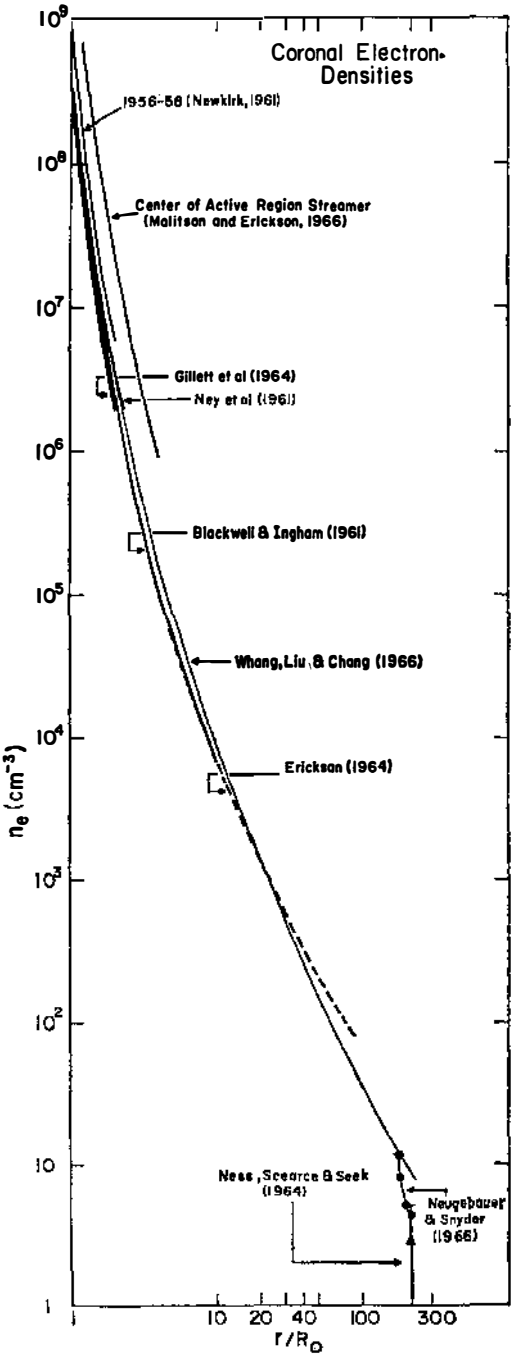

TABLE I

REPRESENTATIVE CORONAL ELECTRON DENSITIES

(Equator at sunspot minimum)

$R(R_\odot)$	$N_e(\text{cm}^{-3})$
1.02	4.0×10^8
1.1	1.4×10^8
1.2	7.0×10^7
1.3	3.7×10^7
1.4	2.3×10^7
1.6	1.0×10^7
2.0	2.8×10^6
2.5	9.0×10^5
3.0	4.0×10^5
4.0	1.2×10^5
6.0	3.1×10^4
8.0	1.3×10^4
10.0	9.8×10^3
15	2.5×10^3
20	1.3×10^3
30	4.6×10^2
50	(1×10^2)
100	(2×10)
215	2.5

Sunspot maximum densities can be expected to be $\simeq$2 times higher. Polar densities are uncertain as are those between 30 and 215 $R_\odot$.

Sun, it is appropriate to examine the accuracy with which the density structure has been established.

Coronal photometry.—Photometric studies during eclipse (for a summary see Hata & Saito 1966) and outside of eclipse by means of sensitive polarimeters (Wlerick & Axtell 1957, Dollfus 1958, Newkirk 1961) yield values of the coronal radiance out to as far as 30 $R_\odot$. The technique for translating the observed radiance and polarization into $n_e(R)$ is quite standard (van de Hulst 1950a) and rests upon the assumption that the K corona is entirely due to the

FIG. 1. A compilation of electron densities in the equatorial solar corona derived from a variety of techniques. No attempt has been made to rectify data made during different portions of the sunspot cycle. A single theoretical model (Whang, Liu & Chang 1966) of the density structure in the solar wind appears for comparison.

Thompson scattering of photospheric radiation by free electrons.[2] Although the technique is straightforward in principle, it is fraught with practical difficulties. Eclipse observations are made against a background of sky radiation $B_{sky} \sim 6 \times 10^{-10}\ B_\odot$ to $2 \times 10^{-9}\ B_\odot$ ($B_\odot$ is the mean radiance of the entire solar disk), which is brighter than the K corona at distances >6–$10\ R_\odot$. Even when high-altitude aircraft, balloon, and satellite observations are employed to reduce the magnitude of this correction, the F corona or inner zodiacal light is still present as an unwanted background for this purpose. Separation of the contributions of K and F coronas is effected by assuming that the radiation of the F corona is unpolarized and symmetric about the plane of the ecliptic. In addition, one assumes the K corona to be the sole source of polarization and, as a first approximation, the polarization to be that expected from a corona symmetric along the line of sight. The effect of these assumptions on the density determinations must be examined in detail.

Separation of the contributions of the F and K coronas is relatively certain out to a distance of $\sim 10\ R_\odot$. Beyond this point, the radiance of the K corona is such a small fraction of the total that even minute polarizations in the F corona, such as the recent calculations of Giese (1961) warn us to expect, would drastically modify the inferred K-component and electron densities. Since present models of the zodiacal light (e.g. Weinberg 1964) are not unique and so do not permit an unambiguous calculation of the polarization to be expected from the F corona, even the most carefully executed observations (e.g. Blackwell & Ingham 1961) cannot yield reliable electron densities beyond $\sim 10\ R_\odot$ except in abnormally bright streamers. To our knowledge measurements in the centers of deep Fraunhofer lines have not been fully exploited to their full capacity to separate the two components.

The recent observation by space-probes (Neugebauer & Snyder 1966) that the solar wind is *always* present suggests that the assumption of symmetry along the line of sight in reducing photometric observations to electron densities is roughly valid for the equatorial regions. However, the well-known appearance of the corona during sunspot minimum indicates that such symmetry over the poles is certainly not present during that part of the solar cycle, if ever. Reductions of photometric measurements for electron densities at high latitude have generally followed the work of van de Hulst (1950a), who used microphotometer tracings made perpendicular to the poles on eclipse plates to estimate the contribution of the lower-latitude corona seen in projection. These analyses have led to the conclusion that electron densities are approximately half the equatorial values at the same height (Allen

[2] Although the presence of an optical continuum from synchrotron radiation from high-energy particles has been suggested (Kellogg & Ney 1959), careful polarization measurements (Ney et al. 1961) show that this mechanism can contribute only an insignificant fraction to the light of the corona. This negative result does not rule out the possibility that some of the optical continuum from dense sporadic condensations or solar flares may be synchrotron radiation; however, its existence has still to be demonstrated.

1963a). However, the fact that such an interpretation is not unique and may be incorrect was demonstrated when Ney and collaborators (1961) found that they could fit their photoelectric observations of both radiance and polarization at sunspot maximum (1959) with a corona absolutely free of electrons above latitude 70°. A similar absence of electrons above 65° latitude could have occurred at the sunspot minimum eclipses of 1952 and 1963 (Gillett et al. 1964). Although the presence of limb brightening over the poles at X-ray wavelengths (Figure 2) suggests that a polar corona does at times exist, we must conclude that quantitative information on high-latitude electron densities is gravely uncertain and that the corresponding density models must be used with great caution.

Radio-source occultations.—Knowledge of electron densities from 10 to 80 $R_\odot$ can be obtained from observation of the occultation of discrete radio sources by the solar corona. The pursuit of these measurements (Hewish 1958, Slee 1961, Vitkevitch 1961, Erickson 1964, Slee 1966) for a variety of radio

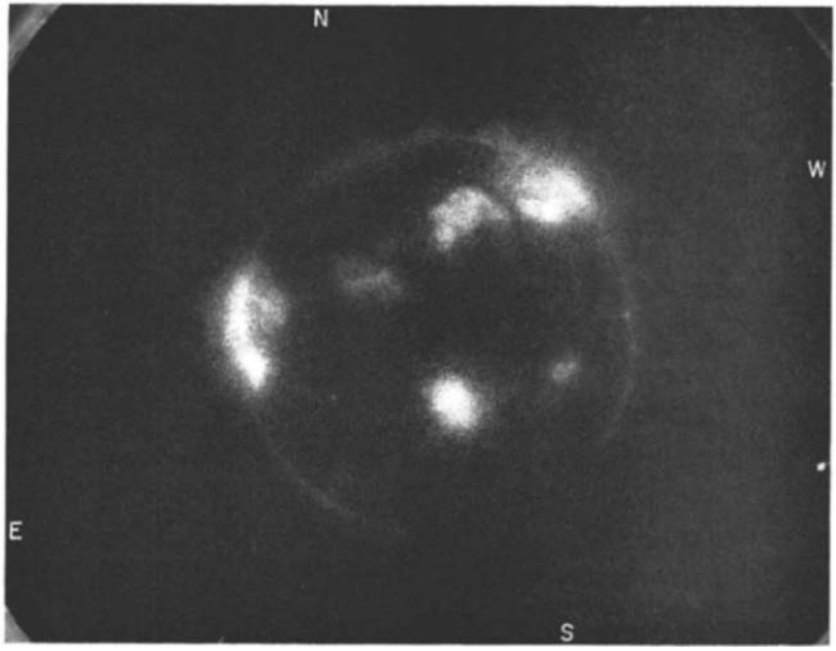

FIG. 2. A photograph of the corona in the wavelength range 27–43 Å, in which the permitted lines of highly ionized atoms contribute most of the radiation. Note the appearance of several X-ray "plages" due to coronal density enhancements, and the outstanding limb brightening. The absence of coronal emission over the southern polar cap compared to that in the north is presumably related to the weak activity which had prevailed in the south for many months prior to the date of observation (20 May 1966). (Courtesy J. Underwood, NASA Goddard Space Flight Center.)

sources over more than a solar cycle has revealed both the shape of the outer corona and its change with solar activity.

Rays from a discrete radio source will be refracted, scattered, and attenuated as they pass through the coronal gas which inevitably contains fluctuations in density about some mean local value. Although in principle the measurement of the amount of refraction would give valuable clues concerning the electron density along the optical path, the ray deviations are so small as to have eluded detection. Of the remaining effects—attentuation and scattering—only the latter as exemplified by the increase in apparent diameter of the radio source has yielded quantitative information concerning the structure of the corona.

The theory of the multiple scattering of radio waves by small density fluctuations in the corona has been developed by Hewish (1955) and Högbom (1960) and recently reviewed by Erickson (1964). In these analyses the outer corona is considered to contain density fluctuations of root-mean-square diameter l and amplitude Δn_e. Although for a completely arbitrary collection of filaments it would be impossible to relate the half-width ϕ_0 of intensity in the scattered radio source to electron density, several simplifying assumptions are possible: (*a*) the effective region of scattering is a thin sector of the corona in the plane of the sky, (*b*) the fluctuation diameter l increases linearly with distance from the Sun, (*c*) the amplitude of the fluctuations and the fraction of space occupied by high and low densities remains constant throughout the corona. It is then possible to show that

$$\phi_0(R) \sim C\nu^{-2}\bar{n}_e(R_{\min}) \qquad 1.$$

in which C is a constant which depends upon such parameters as the amplitude of the fluctuations, ν is the frequency of the radiation, and $\bar{n}_e(R_{\min})$ is the mean electron density at the point of closest approach. Within the limits imposed by these assumptions, Equation 1 allows $\bar{n}_e$ to be estimated directly from measures of $\phi_0(R)$ once the constant of proportionality has been fixed. Thus, by scaling determinations of ϕ_0 at various frequencies according to ν^{-2} and by fitting $\bar{n}_e$ to the Blackwell & Ingham (1961) values in the region 8–10 $R_\odot$, Erickson (1964) has extended the estimates of electron density to 80 $R_\odot$ (Figure 3).

We see (Figure 1) that the densities inferred from this analysis of radio-star occultations appear to be somewhat too high in the outer regions when compared with those measured by interplanetary probes. Clearly, one or more of the assumptions of the model are unrealistic. Probably, most suspect is the assumption that the amplitudes and space-filling factor of the fluctuations remain constant in space. Parker (1964) has found that in a filamented corona with equilibrium between magnetic and gas pressure, the density fluctuations will tend to smooth out with distance. Also, the assumption of a single root-mean-square size is unreliable if a wide range of sizes is, in fact, present or if one scale of irregularities is randomly oriented while another is preferentially radial. We must await further refinement of the powerful tool of radio-source occultations before these ambiguities are resolved.

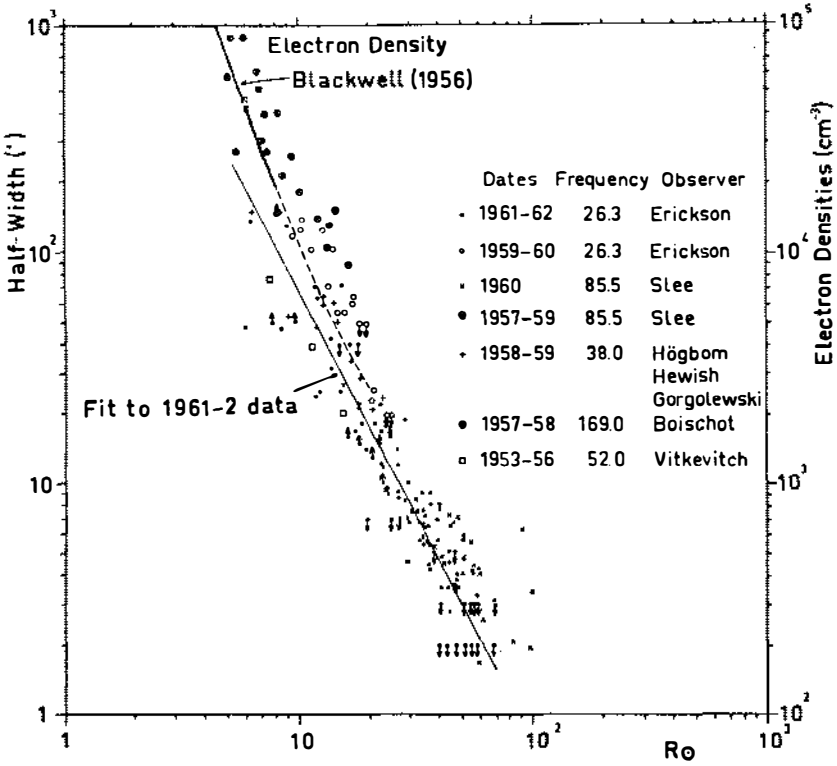

FIG. 3. Electron densities determined from the scattering of the radiation from discrete radio sources occulted by the corona. On the basis of several reasonable assumptions, the scattering half-width is expected to be proportional to $\bar{n}_e$. The factor of proportionality is set by comparison with optically determined densities. (From Erickson 1964.)

Spacecraft measurements.—Although the state of the interplanetary plasma is reviewed elsewhere in this volume (Ness 1967), we include two recent determinations of the density of the corona in the region of 1 a.u. for comparison. During late 1963 (sunspot minimum) a mean value of 3 protons /cm³ was observed (Ness, Scearce & Seek 1963). Detectors aboard Mariner II showed a similar value as well as an increase somewhat more rapid than $1/R^2$ as the spacecraft approached the orbit of Venus (Neugebauer & Snyder 1966). Of course, the difficulty of distinguishing temporal and spatial variations in the latter data prevents definite conclusions concerning the gradient of density of the interplanetary medium.

LOCAL DENSITY STRUCTURE

General morphology.—That the corona possesses an intricate morphology is obvious from its appearance during solar eclipse (Figure 4). Attempts have

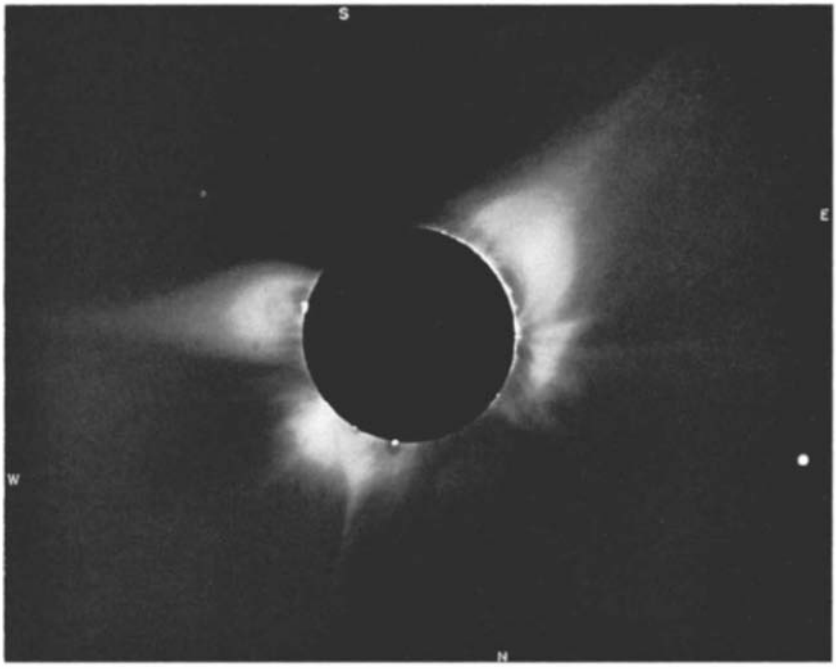

FIG. 4. The solar corona of 12 November 1966 displayed the shape typical of the "intermediate" years of the sunspot cycle. This photograph, made with a radially symmetric, neutral-density filter in the focal plane to compensate for the steep decline of coronal radiance with increasing distance, allows structural features to be traced from the chromosphere out to 4.5 $R_\odot$. The overexposed image of Venus appears in the NE quadrant. Typical "helmet" streamers overlie prominences in the SE and SW quadrants while another streamer at high latitude in the NW develops into a narrow ray at large distance. Arches and the absence of coronal material in the domes immediately above prominences are particularly striking at the bases of the NW and SW streamers. A coronal condensation is visible on the NW limb at a latitude of about 25°. Faint polar plumes over the South Pole represent the typical orientation along the lines of force of a magnetic dipole while those over the North Pole show a much more complex structure. (High Altitude Observatory photograph.)

been made to classify the various forms according to their shape (e.g. Bugoslavskaya 1949) and to associate particular structures with features visible on the solar disk. A classification based on inferences about the geomagnetic effects produced by different coronal structures has been devised by Mustel' (1962a,b; 1964). As one might expect with anything so complex and subtle as the form of the corona, the names used to describe particular features have varied from author to author. Table II displays the reviewer's attempt to form a classification based on earlier works but emphasizing the evolution of coronal forms.

TABLE II

SUMMARY OF CHARACTERISTICS OF CORONAL STRUCTURES

Structure	Diameter at 1 $R_\odot$	Extent in height	Typical density enhancement	Typical density at 1.1 $R_\odot$ (cm^{-3})	Typical temperature (10^6 °K)	Typical age of region	Lifetime	Associated surface feature	Associated coronal emission-line feature	Associated radio, X-ray, and UV feature
Active-region enhancement	200,000 km (5–7 min arc)	200,000 km (0.3 $R_\odot$)	up to 2×	4×10^8	1.5 to 2	2 weeks	2–3 weeks	young active-region plage	green and red line enhancement	"plage"
Active-region streamer	300,000 km (5–7 min arc)	many $R_\odot$	2 to 5×	10^9	2	3 weeks	2–3 weeks			
"Permanent" condensation	50,000 to 130,000 km	80,000 km	$5\times^7$	10^9	2–3	3 weeks	several days	most vigorous active regions, type E sunspot, plage	green and red line enhancement	small bright "button" within plage
Sporadic condensation	20,000 km	20,000 to 80,000 km (may appear as isolated cloud above surface)	50–500×	10^{10}–10^{11}	4–5	3 weeks	fraction of an hour to several hours	often associated with flares and loop prominences	yellow line (5674 Å Ca XIV), continuum	gradual rise at cm radio wavelengths, post-flare enhancements in X rays
Helmet streamer	300,000 km	many $R_\odot$	upper limit of 7–25×	[b]	1.5–2	8 weeks	many months	prominence, extended magnetic fields	?	?
Equatorial streamer	300,000 km	many $R_\odot$	—	$2\text{–}4\times10^8$	1.5–2	?	months to years	15 hours	?	?
Polar plume	30,000 km	many $R_\odot$	4–8×[a]	5×10^8	1.2	?	~ 15 hours	bright polar faculae	?	?
Narrow ray	30,000 km	many $R_\odot$	?	?	?	?	?	?	?	?

[a] Because of uncertainty in true electron densities over the pole, this figure may represent a lower limit.
[b] Density enhancement seldom appears close to surface.

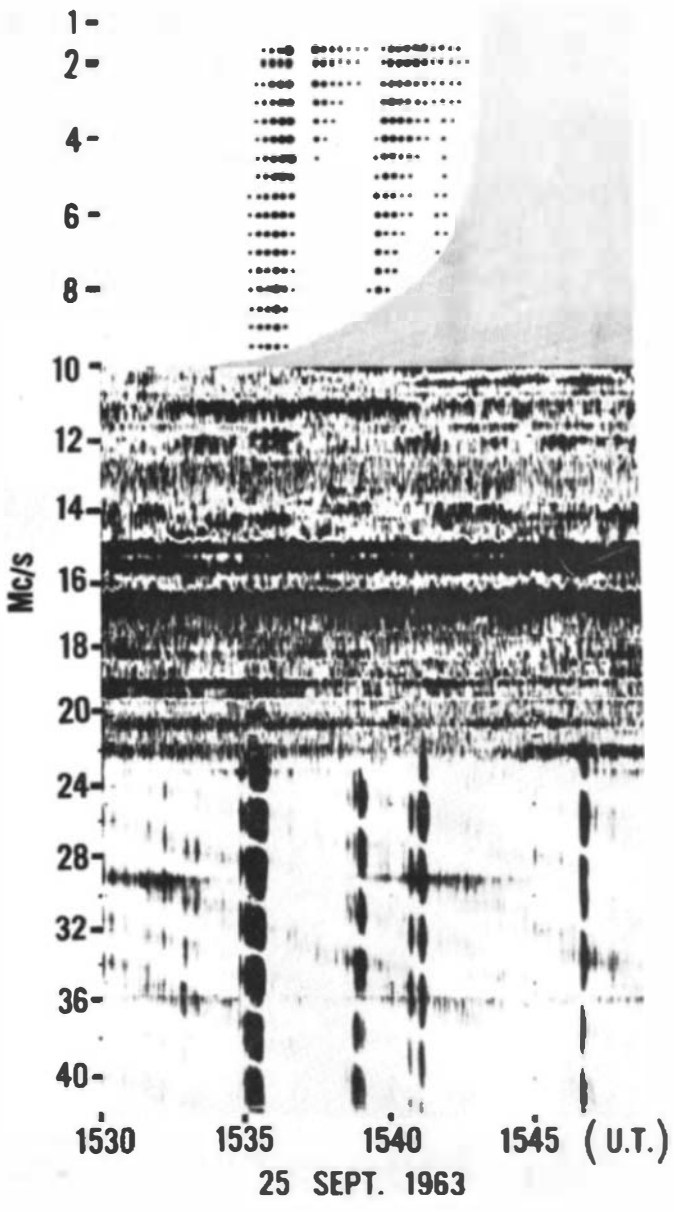

FIG. 5. Type III radio bursts observed from 40 to 22 Mc/s from the ground and from 10 to 1.6 Mc/s from the satellite Alouette I. The frequency range 10–22 Mc/s is obliterated by man-made interference. Periodic breaks in the lower record result from minima in the multilobed interferometer. The drift of the bursts toward lower frequency with time is interpreted as the excitation of plasma oscillations at progressively higher and higher levels in the corona although an independent measure of the heights is required to derive a density model. (From Hartz & Warwick 1966.)

The term "streamer" is taken to refer to the larger structures which appear brighter than the background corona and which extend beyond 0.5 to 1.0 $R_\odot$. Streamers seen over active regions, over the equator, and over prominences (helmets) appear to comprise distinct subclasses. "Enhancement" is reserved to describe the diffuse region of high density which surrounds an active region but which does not extend beyond 0.3 $R_\odot$ above the limb. "Permanent" and "sporadic condensations" were first recognized by Waldmeier & Müller (1950) as smaller-sized density enhancements above active regions while "equatorial streamers" and "polar plumes" have been described at length in the literature (Saito 1958, 1959, 1965a). "Narrow rays" occasionally appear as thin, slightly curved features extending great distances out into the corona.

Densities above active regions.—Densities in the various coronal structures tabulated above are most often expressed in terms of their enhancement above the background or smoothed-out coronal densities at the same height. Unfortunately, two difficulties in the concept remain unresolved: one is never quite sure that the "background" corona may not consist of a collection of unresolved structures such as streamers, thus special attention may be granted only to the truly abnormal features; the location and the extent of the structure along the line of sight are generally unknown so that densities are derived on the basis of some assumption about the three-dimensional shape.

Active-region enhancements appear above plage regions in the coronal emission lines 5303 Å and 6374 Å as well as on K-coronameter and eclipse observations. At X-ray wavelength (Figure 2) and in radioheliograms enhancements may be seen against the disk as well as projected against the sky. These and the more highly developed active-region streamers appear similar to the corresponding plage as seen in K_3 spectroheliograms except that the fine structure is less evident and the edges are more diffuse in the corona. Although little attempt appears to have been made to distinguish between enhancements and active-region streamers, which are in our opinion only two evolutionary stages of the same structure, density increases up to 2× over the background corona appear to be typical (Christiansen et al. 1960, Newkirk 1961, Kundu 1965).

By the time an active region has reached the height of its development 2–4 weeks after its birth, it has produced numerous flares. Accompanying these flares are radio bursts which allow an independent assessment of the electron density. As is well known (Wild, Smerd & Weiss 1963; Maxwell 1965; Warwick 1965), the drift of the radio-noise bursts towards lower frequency with increasing time (Figure 5) is interpreted as the excitation of electromagnetic waves at the plasma frequency (and at times its harmonics) by a disturbance traveling upward through the corona. Type II (slow-frequency drift) bursts are believed to be associated with hydromagnetic shock waves while type III (fast-frequency drift) bursts owe their excitation to a pulse of highly energetic particles. Radio-interferometer measures of the

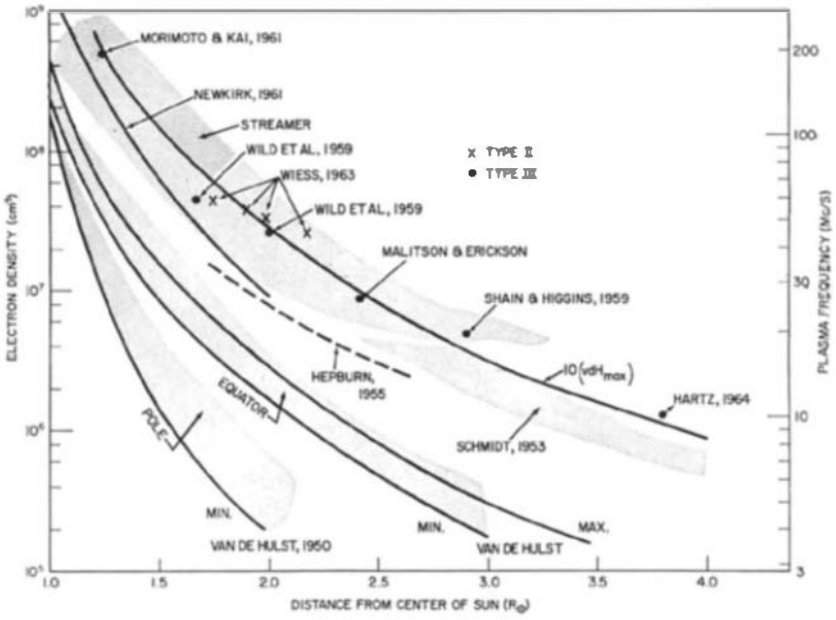

FIG. 6. Radio-burst measurements require electron densities over active regions to be enhanced ~ 10 times those in the model derived for the equator by van de Hulst. The fact that optical observation of streamers (Newkirk, Hepburn & Schmidt) yields slightly lower densities than the radio data is probably caused by the preferential occurrence of bursts in the most active (and most dense) regions. (From Malitson & Erickson 1966.)

heights of the disturbances (Wild, Sheridan & Neylan 1959) give their spatial velocity so that the known-frequency drifts can yield a density model of the corona. Analyses of this type (Maxwell & Thompson 1962, Malitson & Erickson 1966) have been remarkably consistent during the last solar cycle in giving densities above active regions out to 4 $R_\odot$ of 10 times those suggested by van de Hulst (1950a) or Baumbach and Allen (Allen 1963a) for sunspot maximum (Figure 6). Since there is evidence (Newkirk 1961, Ney et al. 1961) that the background corona was some 2 times the van de Hulst values during the last maximum, densities above active regions must have been augmented by a factor of 5 times the background. The height of type III bursts inferred from the statistics of their visibility across the solar disk has been used by Morimoto (1964) to arrive at a similar conclusion.

Initially it might appear that this 5 times augmentation is in disagreement with the factors of 1.5 to 2.5 times found from K-coronameter observations (Newkirk 1961) and from the slowly varying radio component (Christiansen et al. 1960, Kakinuma & Swarup 1962). The difference is presumably real and the result of the biased selection of the most vigorous active regions, and presumably those with the higher densities, by the radio bursts. Chan-

neling of the exciters of type II and type III bursts along the dense axis of the active-region streamers may also contribute to the higher densities suggested by these phenomena. Thus, we conclude that an active region during the stage of its development when flares are present always contains enhanced densities of 2 to 5 times the local background out to at least 4 $R_\odot$.

The structure of "permanent" and "sporadic" condensations was established by Waldmeier & Müller (1950) and has been confirmed on several occasions (Saito & Billings 1964, Kundu 1965) by optical, radio, and X-ray observations. As described schematically by Waldmeier & Müller, the permanent condensation represents a low mound of enhancement ~80,000 km in diameter with densities of $\sim 10^9$ cm^3 at its core. This feature often appears as a substructure within the more extensive active-region streamer. Permanent condensations often contain even denser knots of transitory nature in which the densities (10^{10} to 10^{11} cm^{-3}) are high enough to allow their continuum radiation to be detected on coronagraph spectrograms. These so-called sporadic condensations are intimately associated with loop prominences and the loops and arches seen in coronal emission lines (Kleczek 1963). As with all qualitative descriptions of complex phenomena, one should beware of attaching too much significance to the somewhat arbitrary classification of various types of condensations and to their "typical" characteristics. The intense coronal condensation (Figure 7) observed at the February 1962 eclipse and analyzed by Saito & Billings (1964) amply demonstrates that the distinction between active-region enhancement and permanent condensation is often extremely artificial.

Densities in streamers.—The densities in helmet streamers, which frequently appear above prominences, have been established only by means of optical photometry since, by our definition, these features occur away from active regions and the probing of radio-burst exciters. Although their association with prominences has long been known both statistically and by inference of their true position from the observed polarization (Bugoslavskaya 1949, Schmidt 1953), only a few attempts have been made to distinguish these streamers from others in estimates of density enhancement. Schmidt examined three streamers, two of which could be definitely associated with prominences and the third with a region that had displayed a prominence two months previously; he concluded that densities ~7 times the background occurred. A large streamer observed in 1952 and studied extensively by Hepburn (1955) and Michard (1954) showed negligible enhancement close to the Sun with a rapid increase to 25 or 30 times the background at a height of 3 $R_\odot$. Beyond 3 $R_\odot$ the enhancement above the background corona remained at this very high value. Both these analyses include the assumption that the streamer is roughly cylindrical in form. There is evidence (Saito 1959) that some streamers have considerable extent in longitude and that the inferred enhancements must be considered as upper limits only.

Densities in polar plumes.—Polar plumes can scarcely be discussed outside the context of the variation of the form of the corona with solar cycle. Their striking resemblance to the lines of force about a bar magnet has been

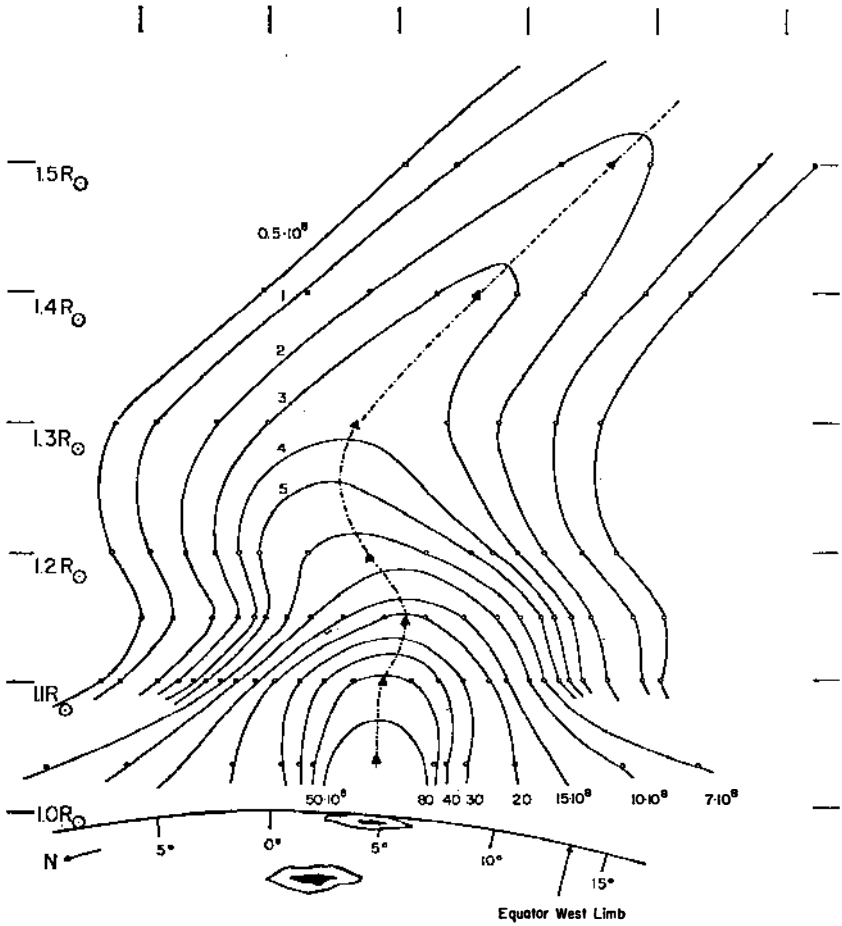

FIG. 7. Electron densities in a coronal condensation derived by Saito & Billings (1964) under the assumption of symmetry about the axis shown as a dot-dashed line. Several isolated loops (not shown) of high-density material appeared within the main structure of the condensation. (From Saito & Billings 1964.)

known for many years, as has the fact that the length of the dipole varies with solar cycle. Since the polar regions of the Sun represent more a patchy collection of magnetic regions than a classical dipole (Severny 1965), it is not surprising that the lines of force outlined by polar rays seldom if ever appear symmetrically about the rotation poles (Godoli 1965). The fact that discrete radio-source occultations show a dipole-like alignment of the scattering irregularities out of 5 to 10 $R_\odot$ (Wyndham 1966) suggests that polar rays maintain their identity far out into the interplanetary medium.

The same analytical tools used to derive coronal densities elsewhere in the

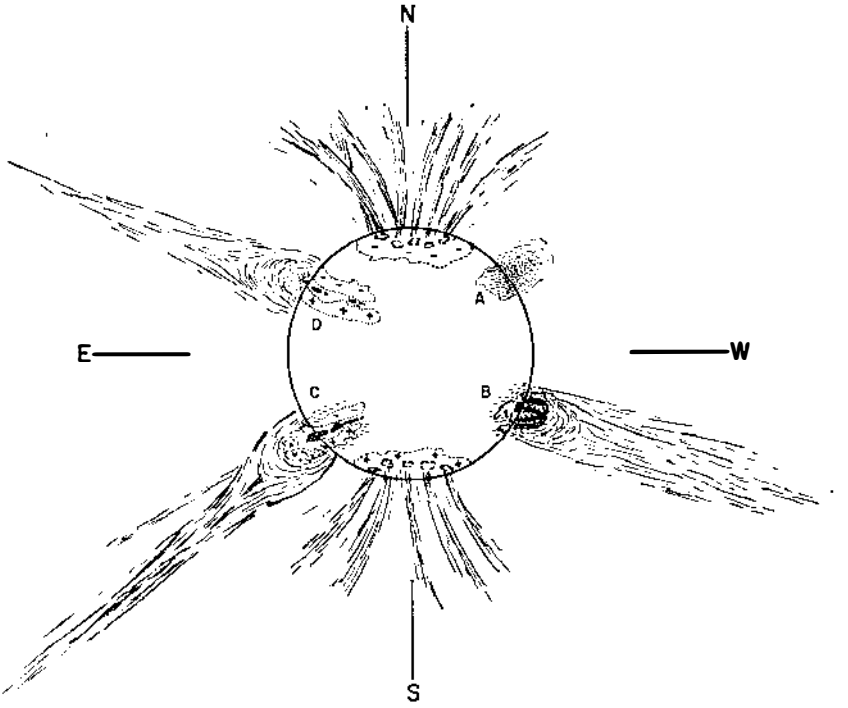

FIG. 8. A schematic representation of the evolution of a "typical" region in the corona from its early appearance as an enhancement (*A*) through the active-region streamer stage (*B*) to the long decline as a helmet streamer (*C* and *D*). Both the helmet and the accompanying filament are believed to require the presence of extended regions of opposite magnetic polarity (schematically shown).

corona yield densities in polar plumes. Although their contrast with the background corona is only 10–20 per cent (van de Hulst 1950b, Saito 1965a), their small line-of-sight extension requires densities a factor of 4 to 8 above the background. Such enhancements of density above the background corona, as well as the observation of Saito (1965a) that the density gradient in polar streamers is less steep than for the background, must always be regarded in the light of our previous discussion of the paucity of our knowledge of the density or even the existence of a general polar corona.

The evolution of coronal structures and their connection with surface features. —Although the necessary data—synoptic observations of the corona out to at least $6R_\odot$—are not available, we can attempt to construct a picture of the evolution of a "typical" active region as it appears in the corona (Figure 8). Immediately following the birth of an active region (*A*) with its plages and emergent magnetic fields, a density enhancement appears in the corona. Presumably the enhancement owes its origin to the increased flow of material

and energy into the corona and a bottling up of the solar wind—both effects induced in the magnetic fields. We know from eclipse, K-coronameter, and X-ray observations that these enhancements seldom extend very far out into the corona.

At the age of 2–4 weeks (*B*) the active region has reached the height of its development (Kiepenheuer 1953) with complex configurations of sunspots, plages, and magnetic fields. In the corona the active-region enhancement has grown and will often include permanent and sporadic condensations of high density, where the local temperature may be elevated to $4–5 \times 10^6$ °K (Billings 1966). Loops in the corona occasionally form. Presumably as the result of bursts of high-energy particles from solar flares, part of the magnetic field has been stretched out to give the characteristic open or "bush" (Bugoslavskaya 1949) appearance of the corona above active regions. High densities now extend far out into the solar system. How much of the material in this active-region streamer partakes of the solar wind is unknown.

Dissipation of the magnetic fields into extended areas of low strength becomes apparent after a month or so has passed (*C*) (Leighton 1964). Lines of force still connect regions of opposite polarity and mold the helmet streamer into its characteristic form and support the filament appearing at its base. Apparently as a result of condensation of cool prominence material out of the corona, a vacancy often appears immediately surrounding the prominence. Although such helmet streamers contain densities well above those of the background corona, their preference for high latitude may well explain their lack of association with geomagnetic activity (Dizer 1963) and prevent their investigation by present space-probes. In the latter stages of development of such a region, differential rotation will have dragged out the underlying magnetic fields in longitude (*D*). The associated streamer will be expected to have a correspondingly great extent in longitude and would be called a fan by many authors. During the many months of lifetime of this stage, the underlying prominence may from time to time disappear without modifying the overlying streamer. As the field decays further, it loses its ability to channel the solar wind into a streamer, which gradually subsides into the background corona.

Little is known concerning the evolution of polar plumes although several recent researches have been devoted to establishing what if any connection exists between them and surface features. Using the statistical distribution of plumes across the polar cap as well as their observed polarizations to infer positions in three dimensions, Saito (1965a,b) concludes that plumes occurred with maximum frequency at latitudes 75°–80° during the sunspot minimum of 1965 and that the pole itself was bare of these features. Even though his polarization measures seem to lack the accuracy required for such a subtle inference of position, the idea is provocative. What connection exists between such a "plume zone" and the interface between the magnetic fields of the polar region and those migrating toward the pole from lower latitudes (Leighton 1964, Hyder 1965a) is unknown.

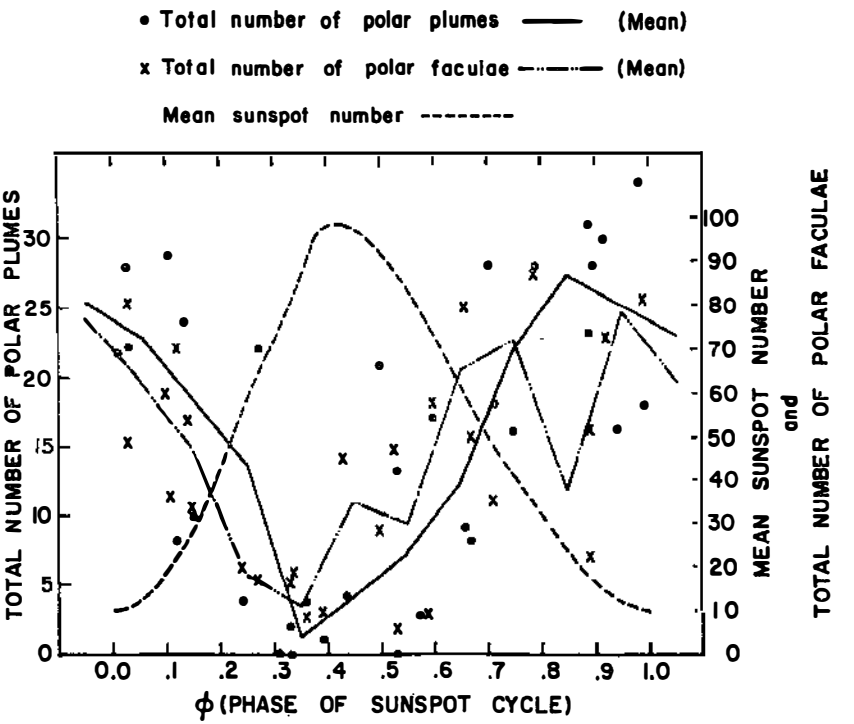

FIG. 9. The number of polar plumes visible on published eclipse photographs (1889–1963) is compared with the number of bright polar faculae (Sheeley 1964) and average sunspot number. Phase in a given sunspot cycle is defined as

$$\phi = \frac{t - t_{\text{preceding min}}}{t_{\text{following min}} - t_{\text{preceding min}}}$$

This and other evidence suggest that plumes originate over the brightest polar faculae.

The association of polar plumes with surface features visible either in white light or in spectroheliograms is difficult to establish for obvious reasons. Bugoslavskaya (1949) states that plumes are rooted on "chromospheric prominences," which would be referred to as large polar spicules by most authors. A distinct correlation between the brightness variation of the north polar corona of 20 July 1963 and that in a polar strip of the K_3 spectroheliogram made the same day has been interpreted by Harvey (1965) as evidence that plumes originate over bright polar faculae. We also note (Figure 9) the similarity between the variation of the number of polar faculae (Sheeley 1964) with sunspot cycle and the number of polar plumes counted from published eclipse photographs extending from 1889 to 1963. The hazards of inferring causal relationships from such statistical evidence are well known; however, if we accept the counts at face value we conclude that, since only half

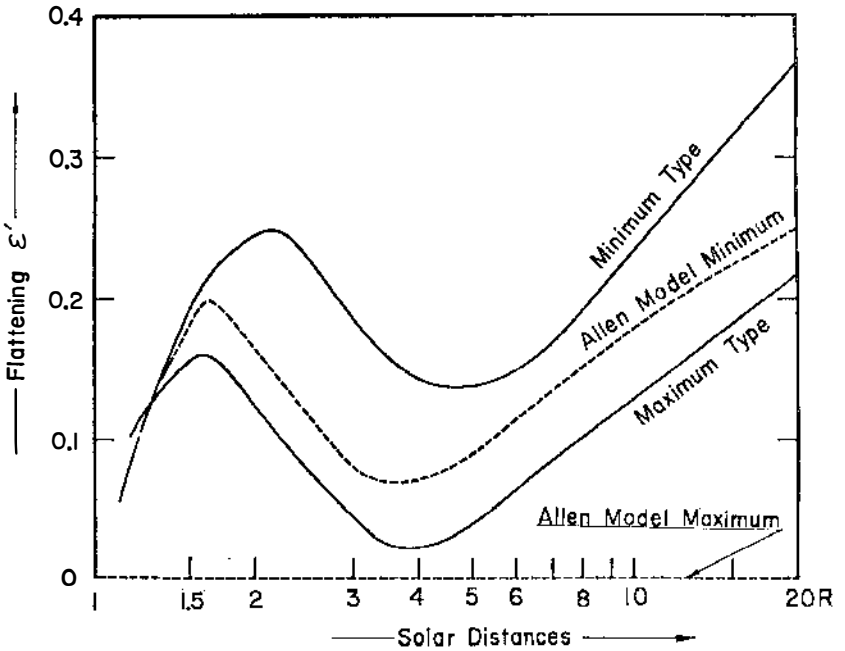

FIG. 10. Variation of the flattening index ϵ' of coronal isophotes with distance. Even at sunspot maximum the corona is not spherically symmetric and a strong concentration at the equator is always apparent. (From Hata & Saito 1966.)

the polar faculae are visible at any one time, only about one in seven faculae possesses a visible polar plume. Thus, these several pieces of data all support the plausible but hardly well-demonstrated conclusion that polar plumes overlie polar faculae, which represent regions of higher material flux into the corona.

Solar-cycle variations in the corona.—The familiar variation of the appearance of the corona with solar cycle has been well documented (van de Hulst 1953) and recently reviewed (Hata & Saito 1966) to include more recent data. A flattening index

$$\epsilon' = \frac{R_{eq}}{R_{pole}} - 1$$

for coronal isophotes allows a large quantity of data to be surveyed at a glance. We note in Figure 10 that the difference between the sunspot minimum and sunspot maximum is one of degree only—both are far from spherically symmetric. Evaluation of the scattering by the corona of the radiation from many discrete radio sources has led Slee (1966) to conclude that the flattening index continues to increase to a value of about 0.7 in the region 20–80 $R_\odot$. Although it is questionable that the shape of the ellipse of

constant scattering can be directly equated to the shape of coronal isophotes, it seems clear that the concentration of the corona toward the equator becomes more exaggerated at large radial distances.

The variation of the innermost corona visible in the 5303 Å line has been described by Waldmeier (1957), who discovered three zones of emission: 1) a dominant maximum which progresses toward the equator with the sunspot zone, 2) a band which originated at about 50° latitude early in the sunspot cycle and reaches the pole at about the time of sunspot maximum, and 3) a zone which appears at high latitude late in the cycle and reaches 40° latitude at about the time the new cycle begins. The behavior of the active-region zone needs little explanation, except that we have only a qualitative explanation (Babcock 1961) for the fundamental processes underlying sunspot activity in general. The similarity between the poleward migrating zone and a similar class of prominences (Kiepenheuer 1953), as well as that of the migrating magnetic regions (Babcock 1961, Leighton 1964), suggests that the magnetic regions are responsible for both phenomena. The origin of the third zone remains an enigma.

Density variations in the corona throughout the last solar cycle have been documented by eclipse photometry [see Hata & Saito (1966) for a review], radio-interferometer observations of the thermal emission of the corona (Kundu 1965), and radio scattering data (Slee 1966, LeSqueren-Malinge 1964, Erickson 1964). A consensus of these various investigations appears to be that electron densities throughout the corona at sunspot maximum are about twice those at sunspot minimum. Comparison of observations made during the last sunspot maximum (Ney et al. 1961, Newkirk 1961) with those of previous maxima (van de Hulst 1953) indicates that an increased level of activity at a given maximum leads to abnormally high electron densities—during 1957–1959 densities of 1.4 to 2 times the van de Hulst model for sunspot maximum were present.

Small-Scale Density Fluctuations

There is overwhelming evidence that the corona possesses, in addition to the gross structural features associated with active regions and streamers, fine-scale fluctuations in density. High-resolution eclipse photographs (e.g., those made by the Swarthmore expedition in 1930) present a corona which appears to have been carefully groomed with a fine comb. Interplanetary probes of the solar wind show a wide spectrum of temporal variations of plasma density and velocity. Such effects as radio-source scattering, interplanetary radio scintillation, diffusion of solar cosmic rays, and radar Doppler displacements in the corona would be nonexistent or vastly different if the corona were a smooth plasma. The presence of such fluctuations also plays a vital role in explaining the excitation of type III radio bursts by high-speed particles (Ginzburg & Zhelezniakov 1958). Finally, comet tails show the results of sudden accelerations due to small-scale structures in the interplanetary medium (Antrack, Biermann & Lüst 1964). Recent investigations have

yielded exciting details concerning the scale, amplitudes, and orientations of these fluctuations in the corona.

The inner corona.—Optical observations of coronal irregularities are intrinsically limited by the fact that the intensity fluctuations produced by small features become lost in the noise of the photographic or photoelectric detector as soon as more than a few features appear along any single line of sight. No quantitative analysis of the spectrum of structure sizes visible on high-resolution coronal photographs has been made although we have determined that the smallest features visible on the Swarthmore plates had a diameter 3×10^3 km—a figure suspiciously close to the resolution limit of the observations. Recent spectroscopic observation of the K line of Ca^+ in emission in the corona out to 0.3 $R_\odot$ has been interpreted by Deutsch & Righini (1964) as due to the presence of dense, cool regions in the corona. Although the necessary insulation of such regions (hypothesized to occupy only 10^{-4} of the coronal volume) by magnetic fields is not impossible, it appears that the basic observation of K line emission from the corona is erroneous—the result of scattered chromospheric radiation by the image-forming optics and the aircraft window.

Small-scale density fluctuations in the lower corona ($\sim$1.3 $R_\odot$) make their presence indirectly known by the diffusion of the radiation from radio-noise bursts. Using a Monte Carlo technique to trace rays from the burst through randomly oriented coronal irregularities, Fokker (1965) has concluded that such scattering can account for the general characteristics of the angular distribution of radiation emerging from bursts in the 200 Mc/sec range. His model does not predict the detailed appearance of these bursts as a bright core surrounded by an extensive halo (Weiss & Sheridan 1962), however. Fokker finds that the magnitude of the scattering in the inner corona is nearly an order of magnitude lower than that found from 10 to 80 $R_\odot$ by radio-source occultations and suggests that the amplitude of the fluctuations must increase in the outer parts of the corona. However, an alternate explanation for this difference must be considered. Erickson (1964) has noted that the observed angular distribution of radiation from an occulted radio source is consistent with scattering elements which are more or less randomly oriented but with a preference for radial alignment. Radiation from a source imbedded in such a corona could thus emerge nearly parallel to most of the density inequalities and experience less scattering than the radiation from an occulted radio star.

The outer corona.—In addition to the estimates of coronal electron densities described earlier, the analysis of discrete radio-source occultations reveals information on the scales and orientations of the density fluctuations. The fact that the corona acts as a polarizer suggests that the fibers over the poles are oriented along the magnetic dipole (Hewish & Wyndham 1963). However, Erickson (1964) finds that the generally radial elongation of scattering elements must still be mixed with a random component to explain the observations.

Using measures of the size ϕ_0 of a diffused radio source alone, one cannot discover the scale of the interplanetary density fluctuations. The same value of the proportionality constant C in Equation 1 may be produced by a few large fluctuations or a great number of small ones. An additional observation —the absence of seeing effects as the rays pass through first one and then another irregularity—is crucial for an estimation of the scale. In a series of papers Hewish (1958), Slee (1961), and Hewish & Wyndham (1963) have attempted to establish an upper limit for the scale of the irregularities from the lack of observed seeing effects with amplitudes larger than 6 sec of arc. They argue that cells of enhanced density of angular diameter larger than the interferometer beam carried through the line of sight by the solar wind would produce temporal variations in the apparent position of the centroid of the scattered source. Since such seeing effects are not observed, they conclude that $l < 5 \times 10^3$ km. Such structures have dimensions of a few hundred kilometers when projected back to the Sun and might be related to chromospheric spicules.

Critics [see discussion following Wyndham (1966)] of this interpretation of the radio-occultation data have noted that while a structure of scale $l \sim 5 \times 10^3$ km may be present and may even be required, the data do not truly rule out the presence of larger features. We note that the crucial absence of seeing effects larger than 6 sec of arc over intervals of several minutes is observed at a separation between the Sun and the source of 80 $R_\odot$. At this distance a ray from a discrete radio source would still intercept and be deflected through small angles by some 20 to 50 irregularities even if their scale were as large as 10^6 km, and the chance that seeing effects could be observed would still be small. Moreover, anticipating the discussion of the section to follow, we find that the larger coronal density irregularities detected by direct space-probe measurements can explain much of the observed radio scattering.

Recent observations of interplanetary scintillations of discrete sources (Hewish, Scott & Wills 1964; Cohen et al. 1966; Vitkevich, Antonova & Vlasov 1966) and of Jupiter (Slee & Higgins 1966) have been interpreted as of interplanetary origin and appear to give support to the presence of small-scale ($l \sim 5 \times 10^3$ km) irregularities in the interplanetary medium. Hewish and collaborators estimate that these small structures move across the line of sight with speeds 50–190 km/s and they conclude that the scintillations are produced as the filaments are swept by the Earth with the rotation of the interplanetary medium. The observed change of scintillation frequency with heliographic latitude lends credence to this argument.

Space-probe measurements.—Direct space-probe measurements provide, of course, the most unambiguous evaluation of density fluctuations in the outer solar corona. Examination of the data relayed by such satellites as Mariner II (Neugebauer & Snyder 1966) reveals long-period increases in density lasting for several days. These stable structures, in which the density may rise to 70 protons/cm^3 as compared to the normal 3 protons/cm^3, often

recur at 27-day intervals and appear to be related to the sectored structure of the interplanetary magnetic field found by Wilcox & Ness (1965). It is not surprising that these large-density structures have appeared in radio-occultation records as abnormal changes in scattering and attenuation of several days' duration (Slee 1961).

Within these large regions of unusually high density, smaller-scale fluctuations appear (Figure 11) which are identified as filamentary structures imbedded in the solar wind. Even when the data are presented as 3-hour averages, density variations by factors of 5 or more frequently occur within 3 to 12 hours' time. Although the small-scale irregularities visualized by the radio observers would be completely masked in these averaged data, it is quite clear that large-amplitude density fluctuations of dimensions as large as 4×10^6 to 2×10^7 km (a mean velocity of 400 km/s is assumed) are quite common in the corona at 1 a.u.

Measurements of the interplanetary magnetic field also allow inferences concerning the detailed density structure of the medium although it must be kept in mind that field and plasma measurements are not one and the same thing. It is well known that the field is remarkably stable in value at 4–7 $\times10^{-5}$ G and exhibits a streaming angle corresponding to an Archimedes spiral for a velocity of 300–700 km/s (Ness, Scearce & Seek 1963). Within this gross alignment the field is observed to reverse sign within periods of 10 minutes up to several hours. From this duration of fields of the same orientation we conclude that the width of a given magnetic bundle is between 3×10^5 and 3×10^6 km. Fluctuations in the field of even shorter duration found by Pioneer VI (Ness, Scearce & Cantarano 1966) are presumed to represent Alfvén waves.

Complementary information concerning the structure of the interplanetary magnetic field is obtained by satellites carrying cosmic-ray detectors outside of the Earth's magnetosphere. It has long been known that cosmic rays produced by solar flares initially arrive at the Earth from the direction of the Sun and only after considerable time do they become isotropic through diffusion within the solar system. Recent measures in the 13-MeV range (Bartley et al. 1966, Fan et al. 1966) show that although the average direction of arrival of the flare protons centers about the streaming angle of the overall interplanetary field, abrupt and large fluctuations in velocity vector occur every 0.5 to 4 hours. The strong correlation (McCracken & Ness 1966) found between the direction of the interplanetary field and that of arrival of the cosmic rays suggests that the particles are being conducted along magnetic tubes of force with overall dimensions of 7×10^5 km to 6×10^6 km. Moreover, the extreme anisotropy of the flux within a given tube as well as the abruptness of the boundaries observed between tubes requires that the magnetic field must be smooth on a scale of 10^5 km, the gyroradius of the particles.

In summarizing the observational aspects of fluctuations of density in the corona we are faced with apparently contradictory evidence. Radio-source occultations and interplanetary scintillations require the presence of struc-

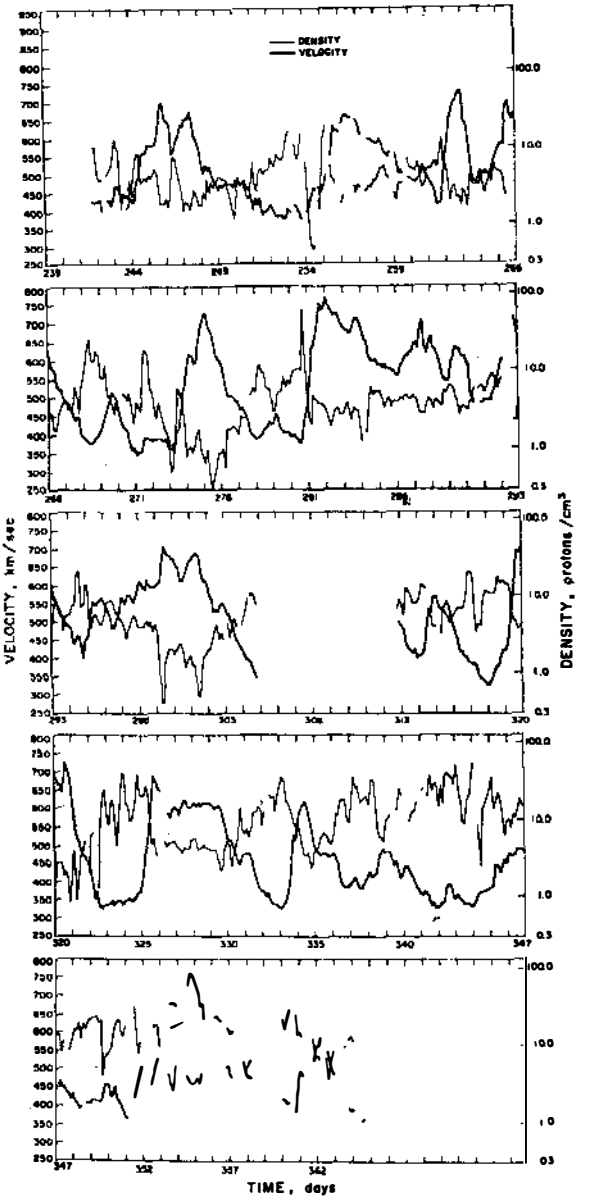

FIG. 11. Variation of the velocity and density of the interplanetary medium as measured by the Mariner II spacecraft and averaged over 3-hour intervals. The occurrence of high velocities with low densities and vice versa is apparent. Rapid changes in density (or velocity) over a few hours' time show that the interplanetary plasma contains density irregularities with a scale of some 10^8 km diameter. (From Neugebauer & Snyder 1966.)

tures with a scale of 5×10^3 km and rule out the existence of fluctuations as large as 10^6 km. On the other hand, direct plasma probes and the inference of density fluctuations from the structure of the interplanetary magnetic field demonstrate unquestionably the presence of structures of dimensions of the order of 10^6 km, and cosmic-ray measurements suggest that irregularities smaller than 10^5 km cannot occur in any great numbers in the entire space between the Sun and the Earth. The contradiction is only partly resolved by the fact that the radio observations are primarily sensitive to the very small and presumably numerous density fluctuations while present space detectors reveal only the larger structures. The cosmic-ray data appear to require that the small-scale density structures, if they exist, have no corresponding structure in the magnetic field.

Origin.—Several origins for density fluctuations in the outer solar corona can be imagined. Certainly some irregularities represent shock waves which develop when a stream of fast particles overtakes a slower stream (Parker 1963). Helmholz instabilities similar to the flapping of flags in the wind will develop at the interface between parallel streams with different velocities. Alfvén waves also undoubtedly occur. Although these various sources of density irregularities bear detailed investigation, the correspondence between solar and interplanetary magnetic fields on a large scale discovered by Wilcox & Ness (1965) suggests that photospheric, magnetic structures of still smaller dimensions may also be carried into the interplanetary gas. In the absence of a quantitative theory for such a conformal mapping, we can only assemble several pieces of circumstantial evidence.

At 1 a.u. the satellite data reveal density fluctuations of a factor of 5 or 10 with scales of 3×10^5 km $< l < 6 \times 10^6$ km. In the inner corona, polar plumes and what few rays can be occasionally discerned over faculae (van de Hulst 1953) have a characteristic diameter of approximately 3×10^4 km (Saito 1965a) and appear to contain densities approximately 5 times the background. We note that radial expansion of coronal irregularities of this size at the Sun would produce features rather close to the dimensions of those observed at 1 a.u. by space-probes. Thus we might envision a corona completely interlaced with tangled filaments which originate over the chromospheric network forming the boundaries of the supergranulation. Magnetic fields present in the network (Howard 1959, Simon & Leighton 1964) serve to constrain the material flowing into the bottom of the corona to individual tubes while the general outward streaming of the solar wind sweeps the filaments out into interplanetary space. Justification for considering the chromospheric network as the origin of these coronal filaments is offered by Kulsrud (1955), de Jager (1962), and Kuperus (1965) who note that the presence of a magnetic field in the photosphere will substantially increase the density as well as the energy flow into the overlying corona. Of course, this model of the detailed mapping of chromospheric magnetic structures out into the corona and interplanetary medium and the origin of whatever filamentary structure exists in the corona is only a plausible hypothesis. A self-consistent picture of

the small-scale structure of the corona and interplanetary plasma will, it is to be hoped, result from future investigations.

Dynamics of Coronal Structures

The steady flux of coronal gas out into interplanetary space amply demonstrates that the corona is a dynamical medium in an approximately steady state rather than a static one. The solar wind with a flux $\sim 5 \times 10^8$ protons/cm^2/s (Ness, Scearce & Seek 1963) demands that the lower corona be replaced about once a day. In addition to the general flow of the solar wind, occasional displacements and oscillations appear in localized regions of the corona. Moreover, at least the inner portion of the corona must share in the rotation of the Sun. We shall first examine the observational evidence for these various dynamic aspects of the corona. Where a well-developed theory exists, as for the solar wind, we shall compare the results with the observations wherever possible, although a complete review of the theory is not intended.

Local macroscopic motions.—Bugoslavskaya's (1949) classical study of the structure of the corona also included an attempt to determine what macroscopic motions occur in various features. Using eclipse photographs made at several stations along the totality path and covering a few hours of elapsed time, she inferred the following magnitudes for the motions:

arches over prominences—2 km/s
helmets—<4 km/s
archlike structures over sunspots—10 km/s
small coronal "clouds"—15 km/s
knots and "clouds" over sunspots—47 km/s
displacements in thin rays—45 km/s
displacements of polar plumes—0.6 km/s
expansion of outer limits of streamers (fans)—1 km/s

However, since position measurements of diffuse coronal features to an accuracy of better than several seconds of arc are extremely difficult, the velocities of only a few km/s must be regarded with caution. Motion pictures in the 5303 Å line show velocities of tens of km/s for the emergence of coronal loops above sunspots (Kleczek 1963), as well as speeds of 600 km/s in the violent release of one end of the loop, to create a coronal "whip" (Evans 1957). That such motions represent real displacements of the material was questioned by Lyot (1944), who concluded that most of the apparent transverse movement in emission-line regions was an illusion created by traveling zones of excitation or the successive growth and decay of adjacent structures.

Of course, no such ambiguity afflicts measurements of the Doppler displacement of coronal emission lines. Waldmeier (1947) and Dollfus (1957) have found that, except over active regions, these velocities seldom exceeded a few km/s. However, in the dense and hot sporadic condensations, which often appear as intense loops in 5303 Å, speeds of up to 150 km/s occur. A detailed examination (Newkirk 1957, Karimov 1961) of Doppler motions in

6374 Å (Fe X) and Hα from such regions shows that although the coronal ions generally travel in the same direction as the neutral hydrogen in the associated loop prominence, the average speed of the coronal material is much lower. Those few instances in which the velocities are equal appear to be associated with the rapid expansion of the coronal and prominence loop. For material streaming along the magnetic lines of force, the speeds of coronal ions and hydrogen were found to be in the ratio $v_C/v_H \sim 0.28$. Apparently, electrical forces, which impart accelerations proportional to the ratio of particle charge and mass, play a larger role than gravity in the flow along such loops.

Oscillations.—Observations of macroscopic oscillations in the solar corona are meager. Billings (1959a,b) interpreted a quasi-periodic variation of the width of the 5303 Å line with height above the chromosphere as evidence for the presence of a transverse hydromagnetic wave. More recently Lilliequist (1966) has analyzed a long time-series of spectrograms of an isolated coronal condensation. Genuine fluctuations in both the intensity and width of 5303 Å appear with periods of 150 and 300 sec. A similar periodicity at 490 sec appears in the 6374 Å line. Variations in the intensity of 5303 Å as far out as 1.25 $R_\odot$ have also been detected by Noxon (1966) at an estimated period of 500 sec. Although the cause of these oscillations is unknown, one might speculate that they represent a modulation of the corona driven by oscillations (Evans, Michard & Servajean 1963) of the underlying chromosphere.

Rotation.—Intuition suggests that the inner solar corona must rotate synchronously with the underlying surface; magnetic fields undoubtedly penetrate into the lower regions with sufficient strength to drag the plasma along. Naturally, a point must be reached further out in the corona where the fields are incapable of maintaining rigid rotation and where a given parcel of material begins to lag behind the solar surface. Still further out in the interplanetary medium the gas must follow the classical "garden-hose" trajectory, which closely resembles the Archimedes spiral. To avoid confusion we shall refer to rotation in the innermost region as *rigid rotation* while the term *co-rotation* is reserved to describe the Archimedes spiral region.

Since even the most accurate measures of coronal emission lines are ineffective in determining the rotation of the inner corona, our knowledge is based almost exclusively on the apparent motions of coronal features. Minute systematic shifts visible on her eclipse plates led Bugoslavskaya (1949) to conclude that the corona does rotate with the rest of the Sun. Waldmeier (1950) and Trellis (1957) followed the recurrent passage of regions of bright 5303 Å emission over the solar limbs to determine the rotation rate as a function of latitude. Cooper & Billings (1962) were able to follow one such high-latitude region for over two years to estimate the period at latitude 65°. These data and the more recent rotation rates determined by Hansen & Hansen (1966) from autocorrelation analyses of K-coronameter observations appear in Figure 12 together with estimates of the rotation rate of filaments (d'Azambuja & d'Azambuja 1948), sunspots (Allen 1963a) and polar faculae

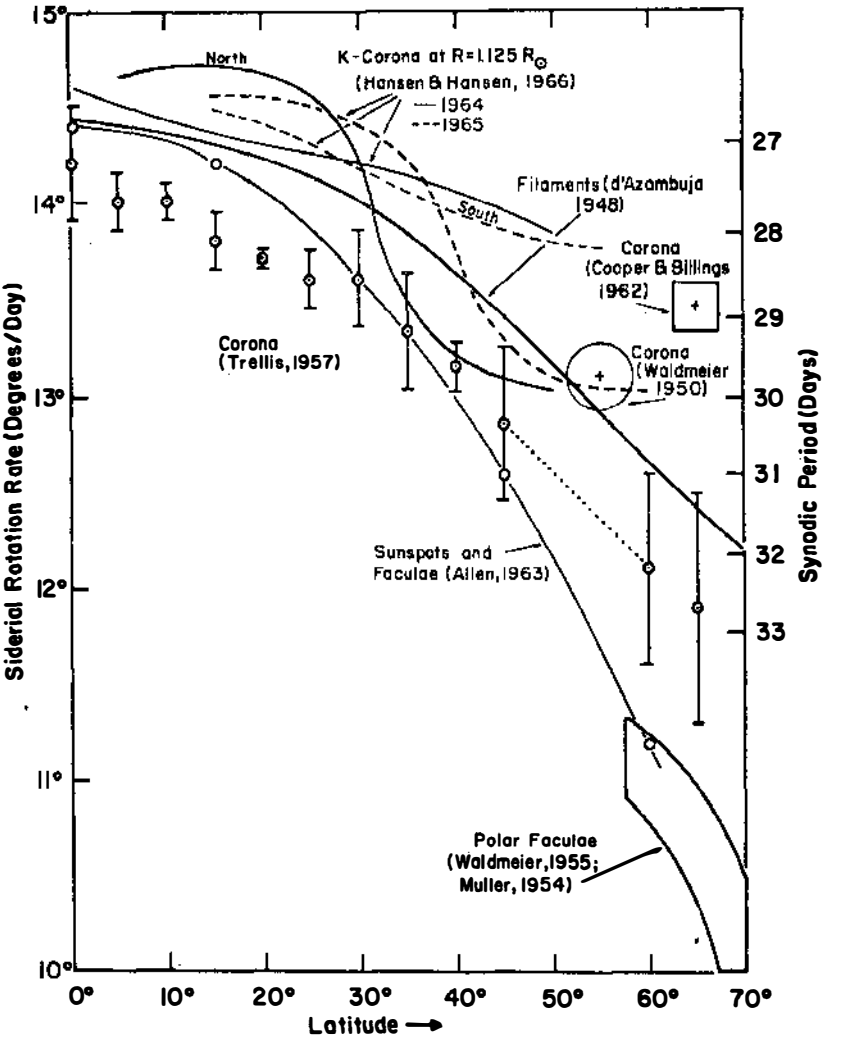

FIG. 12. A compilation of data on the rotation rate of the inner solar corona compared to that of filaments, polar faculae, and sunspots and faculae. (Courtesy R. T. Hansen & S. Hansen.)

(Waldmeier 1955, Müller 1954). While some of these observations appear to suggest that the corona below 1.25 $R_\odot$ rotates with the underlying magnetic fields as revealed by filaments, the Southern Hemisphere data of Hansen & Hansen and of Cooper & Billings require the corona to rotate *faster* than the surface. This apparently anomalous behavior may be produced by dominant

magnetic fields at lower latitude dragging along the higher-latitude corona. However, the comparison of data on coronal and surface features gathered during different solar cycles or inconsistent portions of the same cycle may well yield misleading results. Concomitant information would actually be required to resolve the question.

Rigid rotation of the solar corona out to some distance is of interest not only for its implications concerning coronal magnetic fields but also for its bearing on the evolution of the Sun and similar stars. As has been pointed out by Brandt (1966), the slinging off of coronal gas at the present rate at a rigid radius arm of 30 $R_\odot$ could slow down solar rotation with a characteristic time of only 7×10^9 years. The torque exerted by the outflow of gas from stars with more active chromospheres (Wilson 1966), and presumably higher stellar-wind fluxes, could have a profound influence on the evolutionary track followed by such stars.

The first calculations of the limit of rigid rotation (Lüst & Schlüter 1955) were made on the basis of a static corona containing the imbedded dipole field of the Sun. Distortion of the field by streams of corpuscles to form "magnetic bottles" was later suggested by Gold (1959) as the mechanism by which solar cosmic rays are conducted to the neighborhood of the Earth. Rigid rotation in both models extended out to 20–100 $R_\odot$. Recently, Pneuman (1966a) has examined the detailed interaction of the solar wind with the dipole field to determine the expected variation of solar-wind velocity with latitude and the configuration of the distended field. Using the conclusion that beyond a few solar radii the field becomes approximately radial, he has extended the analysis to include the rotation of the Sun and to estimate the variation of the angular velocity of the equatorial corona as a function of distance. His calculation shows that for a surface field strength of 1 G, rigid rotation extends out to ~ 3 $R_\odot$, above which the angular velocity rapidly approaches that given by conservation of angular momentum. For a surface field of 0.1 G, rigid rotation reaches to only 2 $R_\odot$.

Two basic measurements allow us to estimate the radius of rigid rotation of the corona: the tangential velocity of the solar wind and the curvature of coronal streamers. Although in principle spacecraft observations of the direction of arrival of the solar plasma could yield a value of the tangential velocity, the detailed observations obtained with Pioneer VI show a variation of aberration angle from 8° west ecliptic longitude for particles of 1600 eV per unit charge to about 4° east ecliptic longitude for particles of 600 eV per unit charge. Wolfe et al. (1966) interpret these results as the sum of the *radial* motion of the plasma and a thermal anisotropy of the ions, which have a larger temperature along the magnetic field. They imply that the tangential motion imparted to the ions at the Sun has been masked by the channeling by the magnetic field.

Biermann and his collaborators (Biermann 1951, 1957; Antrack, Bermann & Lüst 1964; Biermann & Lüst 1966) have long recognized that the orientation of ionic tails of comets provides a valuable tool for study of the

solar wind throughout the inner parts of the solar system. Since such tails are believed to be swept back from the head of the comet by the solar plasma and its entangled magnetic fields, the alignment of the tail simply represents the vector difference of the solar-wind velocity and the known velocity of the comet. Although the study of many such comet tails leads to reasonable values for the radial component of the solar wind, this analysis could establish only an upper limit of 20 km/s for the tangential component. Recently, Brandt, Belton & Stevens (1966) have completed an exhaustive study of the orientation of ionic tails of retrograde and direct comets at approximately the same distance from the Sun. This comparison yields a value of ~10 km/s for the tangential velocity of the solar wind at 1 a.u. and requires that rigid rotation must occur out to 32 $R_\odot$. Unfortunately, this estimate is based on data from only a few paired comets with similar but opposing orbital velocities. The errors in the inferred tangential velocity are thus expected to be large although they are not stated by the authors.

Using a unique series of observations of the intermediate corona, from the eclipse of 30 May 1965, from two flights of a balloon-borne coronagraph (Newkirk & Bohlin 1963, 1964, 1965), and from nearly daily coverage by K coronameter, Bohlin, Hansen & Newkirk (1966) were able to estimate the three-dimensional structure of a single helmet streamer from immediately above the surface out to ~5 $R_\odot$. As shown in Figure 13, the projection of this streamer on the plane of the solar equator exhibits the garden-hose curvature and leaves little doubt that rigid rotation dose not extend out as far as 5 $R_\odot$. An attempt to make a self-consistent model of this streamer, including the run of solar-wind velocity with distance, has led these authors to conclude that rigid rotation in this structure extended to between 2.2 and 2.6 $R_\odot$ in remarkable agreement with the calculations of Pneuman.

Certainly, the existence of estimates of the radius of rigid rotation differing by an order of magnitude does not lead to confidence that the problem is thoroughly understood. However, the above data and those presented in our review of coronal magnetic fields suggest that rigid rotation beyond a few solar radii does not occur. Of course, co-rotation of coronal structures with appropriate curvature extends out into interplanetary space until the solar wind becomes overpowered by interstellar magnetic fields at some 50 to 100 a.u. (Axford, Dessler & Gottlieb 1963).

The solar wind.—Scholars of the history of science cannot but be intrigued by the story of the solar wind. Although the presence of streams of corpuscles from the Sun had been known for many years (Chapman & Bartels 1940), the discovery of the solar wind as a continuous outflow of coronal gas is properly attributed to Biermann (1951, 1957), who found that radiation pressure alone could not account for the behavior of many comet tails. Soon after Chapman (1957) pointed out that conduction of energy from the lower corona maintains the interplanetary plasma at 1 a.u. at a temperature of ~200,000 °K, Parker (1958) demonstrated the inevitability of a steady-state solar wind. Parker's ideas were challenged by Chamberlain (1960, 1961), who

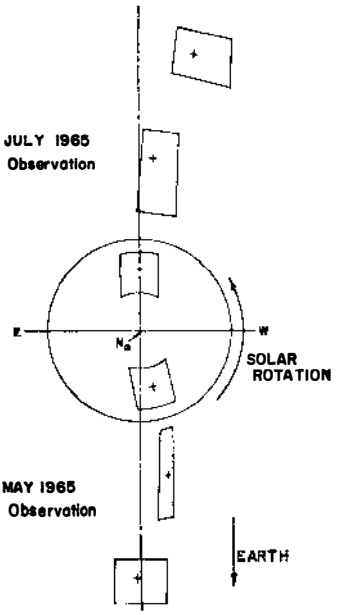

FIG. 13. Detection of a high-latitude helmet streamer over the pole during two meridian passages reveals the "garden-hose curvature" of the feature projected against the plane of the solar equator. Crosses mark the estimated location of the axis of the streamer while the boxes indicate the uncertainty. Such observations can yield data on the velocity structure of the inner solar wind and the height of rigid coronal rotation. (From Bohlin, Hansen & Newkirk 1966.)

claimed that subsonic solutions to the hydrodynamical equations could also satisfy the boundary condition of zero pressure at infinity and that a "solar breeze" was more representative of the corona.

The controversy was resolved in favor of the supersonic solar wind by the first direct space-probe measurements, which showed the velocity of the plasma to be ~400 km/s. Recent studies (Noble & Scarf 1963; Scarf & Noble 1965; Whang, Liu & Chang 1966) have refined the theory of the solar wind while increasingly more sophisticated space-probes have revealed subtle (and often bewildering) details of its structure. Since excellent reviews (Lüst 1962, de Jager 1962, Parker 1965a) of the physics of the solar wind are available, this report will be largely restricted to a comparison of measurements of the solar wind with the various theoretical models rather than a discussion of the subtleties of the theory.

Unfortunately, determinations of the velocity of the inner solar wind are few and often ambiguous. One of the earliest attempts to describe the outflow of coronal gas from the Sun was that of van de Hulst (1950b), who examined the density distribution in polar plumes. Using dynamical equa-

tions including only the initial upward velocity of the material and gravity, he concluded that a significant flow did not exist. Measurements of the outward motion of distinct coronal features by Bugoslavskaya (1949) cannot be readily interpreted in terms of the velocity of the solar wind. One might expect to observe transient changes in the flow of gas in isolated tubes such as polar plumes. However, a recent series of photographs covering nearly two hours of elapsed time from the High Altitude Observatory expeditions at the 1963 eclipse failed to reveal any such events. Several attempts (e.g. Saito 1959) have been made to discover the variation with height of solar-wind velocity using the observed density distribution, cross-section area of coronal streamers, and equation of continuity. The velocity scale is fixed by comparison with the measured value at 1 a.u. This approach is invalid since the shape of the streamer cannot be identified with the flow lines of the material (see later discussion of interaction of magnetic field and solar wind).

Indirect inference of the velocity of the inner solar wind may be made from determinations of the temperature and temperature gradient in the corona and the solution of the appropriate hydrodynamic equations. Billings & Lilliequist (1963) employed measurements of the profile of the 5303 Å line in stable coronal features to estimate a temperature gradient of 3°K/km between 1.03 and 1.82 $R_\odot$. Using the base temperature of 2.6×10^6 °K at $1.03R_\odot$, they derive the velocities shown in Figure 14.

In spite of their low contrast, polar plumes, considered as magnetically isolated tubes of gas, appear to present an ideal opportunity for study of the solar wind since the density gradient can be established unambiguously. Unfortunately, as was shown by Saito (1965a), an independent estimate of temperature gradient is required for numerical solution of the dynamical equations for the velocity. His upper limits (Figure 14) were obtained using a gradient of 3°K/km.

Although radar measurements of the solar corona at present allow the only direct determination of the velocity of the inner solar wind, these reflections are so complex that a simple interpretation of the results is impossible. Chisholm, James, and their collaborators (Chisholm & James 1964, James 1966) find an average returned radar signal with a mean frequency shift of ~4 kc/s (16 km/s) and a spread between half-power points of 25–40 kc/s. The time delay between transmitted and reflected signals leads to a calculated reflection level between 1.05 and 1.25 $R_\odot$ although a spread of nearly 0.6 $R_\odot$ appears always to be present. Often reflections are received with frequency shifts of 60 kc/s (240 km/s) at ranges corresponding to heights of several solar radii. The above observers conclude that the corona at a radar frequency of 38 mc/s must resemble a spiny Christmas tree ornament from which occasional specular reflections with various velocities are seen.

Unfortunately, a consistent model of the corona capable of explaining the complex array of observed Doppler displacements, ranges, and cross sections does not exist. Thus the interpretation to be placed on such a parameter as the mean displacement of 4 kc/s is uncertain. Brandt (1964) has noted that,

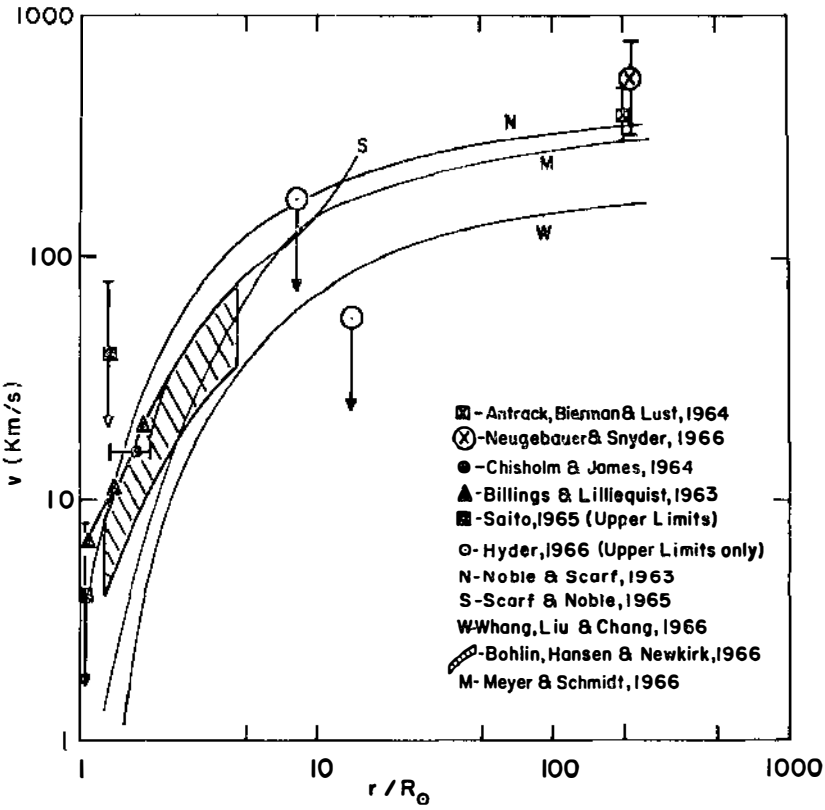

FIG. 14. Estimates of the velocity of the solar wind at various distances compared with several theoretical models.

even if we take this velocity at its face value, lack of knowledge as to how many streamers may be present and whether the streamers contain higher or lower than average solar-wind velocities only allows the reflection level to be placed between 1.7 and 2.0 $R_\odot$. Using a Baumbach-Allen model containing random density irregularities, Chisholm & James suggest a mean reflection level of 1.5 $R_\odot$. The mean outward velocity is represented in Figure 14 with range lines in height to represent these uncertainties. Until it is known how much of the spread in Doppler displacements is due to actual dispersion in the velocity of the solar wind and how much is due to the presence of plasma waves and anomalous reflection effects at density irregularities, corresponding range lines cannot be placed in the velocity coordinate.

Another indirect estimate of the distribution of velocity in the solar wind close to the Sun has been made by Bohlin, Hansen & Newkirk (1966) from the garden-hose curvature observed in a single high-latitude streamer (Figure

13). The requirement that the velocity structure be consistent with both the observed curvature and the fluxes detected at 1 a.u. allows velocities in the cross-hatched area of Figure 14. This estimate is subject to the criticism that an initially radial orientation for the base of the streamer must be assumed and that the outermost portion of the streamer admittedly is poorly located. Moreover, we are still uncertain of how representative the velocities in such a streamer are of the general corona.

As mentioned earlier, study of the interaction of the solar wind with ionic comet tails not only brought about the discovery of the solar wind, but still provides valuable information in the interplanetary medium. Extensive analysis of the aberration of type I tails has led Antrack, Biermann & Lüst (1964) and Brandt, Belton & Stevens (1966) to conclude that at 1 a.u. the mean velocity of the solar wind is ~375 km/s. Individual comets yield values ranging between 300 and 500 km/s with the higher velocities associated with periods of high geomagnetic activity in a manner similar to that observed by space-probes (Neugebauer & Snyder 1966). Moreover, the observed accelerations of material in the tail are frequently found to fluctuate considerably as a result of the patchy structure of the interplanetary plasma. Although comets often penetrate the inner reaches of the solar system, presently published analyses have not been able to describe the variation of the solar wind with distance. The Sun-grazing comet Ikeya-Seki (1965f) appeared to hold promise as a close-in solar probe until it failed to develop an ion tail. However, using measurements of the polarization in the sodium D lines, Hyder (1966a) has attempted to infer the orientation of the cometary magnetic field, which he presumes to be the interplanetary field swept up by the comet. The fact that the inferred field is apparently parallel to the velocity vector of the comet sets the upper limits for the solar-wind velocity at 8 and 14 $R_\odot$ at 175 and 56 km/s at high solar latitudes.

Direct measurements of the solar-wind velocity by space-probes are discussed in detail elsewhere in this volume (Ness 1967) and need not be repeated in detail. The mean velocity observed during the last few years (Coleman et al. 1962, Neugebauer & Snyder 1966) was 500 km/s with values between 300 and 800 km/s appearing frequently.

Theoretical descriptions of the stationary expansion of the corona into interplanetary space are all based on solutions of the equation of motion

$$\frac{1}{N}\frac{dN}{dR} + \frac{1}{T}\frac{dT}{dR} = -\frac{\mu}{kT}\left(g - v\frac{dv}{dR}\right) \qquad 2.$$

where

μ = mean molecular weight of the plasma

$g = g_0\left(\frac{R_\odot}{R}\right)^2$ = local gravitational acceleration

and the other symbols have their conventional meaning. Except for such special circumstances as the influence of the magnetic field on the solar wind

(Pneuman 1966a), authors have uniformly coupled Equation 2 with the equation of continuity for radial expansion. Parker's (1963) early solutions of this equation were made by replacing the temperature term by that for a polytropic gas, for which

$$T = T_0 \left(\frac{N}{N_0}\right)^{\alpha-1} \qquad 3.$$

in which T_0 and N_0 represent the conditions at some reference level low in the corona and α is the polytropic index. Although the use of the polytropic law is somewhat artificial, his solutions for a variety of indices contributed greatly to our insight into just how the solar wind responds to a variety of conditions in the lower corona. Noble & Scarf (1963) discarded the arbitrary assumption of a particular temperature variation by calculating the observed temperature distribution which would be produced by conduction of heat outward from a thin shell low in the corona. They later (Scarf & Nobel 1965) included the effects of kinematic viscosity in the equations, only to find that the added complexity produced instabilities in the numerical solution. A similar model was constructed by Whang, Liu & Chang (1966), who carried out the integration of the equations from far out in the solar system inward towards the Sun. Note that one basic criterion for all these models—their ability to reproduce the observed density distribution (Figure 1)—was particularly well met by the latter calculation. Unfortunately, Whang, Liu & Chang's computed mean velocity of 165 km/s at 1 a.u. fell far short of the observed value. Recently, Meyer & Schmidt (1966) have pointed out that although the model calculated by Whang and collaborators is basically correct, the presence of a radial magnetic field throughout the interplanetary gas so inhibits the transfer of ions from one radial line to another that the effects of viscosity are made negligible. This change scarcely influences the density distribution but brings the calculated velocities into closer agreement with those observed.

In summarizing present knowledge we note that although the broad outlines of the solar wind near the Sun may now be described, the data are scarcely accurate enough to select one of the theoretical models as preferable. Many other unsolved problems confront us. Although space-probes show the solar wind to exist over the entire Sun at low latitudes, we are ignorant of how the flow varies from streamer to interstreamer regions. The evolution of the flow from an active region as the latter develops and decays is unknown, as is the connection between the temperature and magnetic structure of such a region and the flux of the solar wind. Coronal streamers—perhaps the most characteristic structure of the corona—undoubtedly owe their form to the interaction of the solar wind and the underlying magnetic fields; however, we still lack a quantitative theory of their formation. The embarrassing riches provided by space-probe measurements are largely unexplained. The connection between the velocity, density, and magnetic features in the interplanetary medium and visible features in the corona excites the imagination with hypotheses that only the coming years of research will prove or disprove.

Temperature Structure

The quiet corona.—Although our major concern is with the structure of the corona, some discussion of its temperature is still required. Particular attention will be paid to the temperature gradient and its influence on the solar wind, as well as the characteristic temperatures of various morphological structures, rather than the details of different methods of estimating coronal temperatures. It is well to bear in mind that local thermodynamic equilibrium does not exist in the corona and that the entire concept of "temperature" is often illusive. Careful distinction between excitation, ionization, and kinetic temperature is required, although for lack of a complete theory we are forced to treat them as equivalent in our discussion. For a review of the problems attendant on determining the temperature of the corona, the reader is referred to the recent books of Billings (1966) and Zirin (1966) and the treatise of Shklovsky (1965).

The discrepancies which plagued the evaluation of temperature in the lower corona are familiar (Seaton 1962). Estimates from the observed density gradient with the assumption of hydrostatic equilibrium (Hepburn 1955, Pottasch 1960, Ney et al. 1961, Saito 1965a) yielded values of the kinetic temperature of electrons of $\sim 1.5 \times 10^6$; widths of the 5303 Å line led to a somewhat higher $T_i \sim 2 \times 10^6$ °K for the kinetic temperature of ions, while the equilibrium implied by the observed intensities of coronal emission lines demanded ionization-excitation temperatures in the 5×10^5 to 8×10^5 °K range. Some interpretations of the thermal radio emission of the corona (Allen 1963b) appeared to favor a lower electron temperature while detailed studies of the radio spectrum in combination with simultaneous optical measures of coronal density were consistent with kinetic temperatures of 1 to 2×10^6 °K (Christiansen et al. 1960, Newkirk 1961). Recent investigations have largely removed these discrepancies. Burgess (1964, 1965) has found that the mechanism of di-electronic recombination is vastly more important in the equilibrium of coronal ions than had previously been suspected, and that the new ionization cross sections lead to ionization temperatures of about 2×10^6 °K. Although the radio fluxes in the centimetric and decimetric range are roughly consistent with a similar value for the kinetic temperature of electrons (Kundu 1965), quiet-Sun fluxes at wavelengths of 1–10 m still appear lower than could be explained by reasonable density models. Recently, Oster & Sofia (1965) have pointed out that dispersion of radio waves near the plasma frequency has a profound effect on the opacity of the plasma and that brightness temperatures 0.3 to 0.6 as great as the electron temperatures must be expected at these longer wavelengths. The somewhat higher kinetic temperatures required by the widths of coronal lines have frequently been ascribed to the presence of macroscopic turbulence. Billings (1965) has pointed out that the turbulent radial velocities of 35 km/s apparent from Doppler radar observations of the Sun (Chisholm & James 1964) rather nicely account for the unusual width of the 5303 Å line seen at the limb. Thus, we must conclude that in general the lower corona can be re-

garded as maintaining a "temperature" of approximately 1.5×10^6 °K with, perhaps, an increase by 20 per cent during sunspot maximum (Waldmeier 1963). Electron temperatures in polar plumes (Saito 1965a) appear to be somewhat lower—1.2×10^6 °K. On the basis of the heating of the lower corona by shock waves, Kuperus (1965) finds roughly similar values.

Active regions.—Detailed temperature structure is evident in the corona above active regions (Table II). Linewidths in active-region enhancements suggest elevated kinetic temperatures of up to 2×10^6 °K (Billings 1966). The observed brightness temperatures associated with the slowly varying component of radio emission (Kundu 1965, Newkirk 1961, Kakinuma & Swarup 1962) yield similar values when account is taken of the increased opacity of the plasma in such regions due to the mechanism of magnetoionic resonance (Zhelezniakov 1962). Likewise the coronal "plages" visible at X-ray wavelengths suggest brightness temperatures of 1.8 to 2.3×10^6 °K (Acton 1966).

Even higher temperatures appear in permanent and sporadic condensations, which appear as small bright knots in both X-ray and decimetric radio observations and as the source of 5694 Å emission in the optical region. Indeed, such regions at brightness temperatures of from 3 to 5×10^6 °K account for a major fraction of the X-ray radiation of the Sun (Mandelshtam 1964, Acton 1966, Widing 1966). Although some authors have suggested temperatures higher than 10^7 °K to account for the bursts of microwave radiation received from sporadic condensations (Kawabata 1963), it appears likely that the concept of temperature is inappropriate for such phenomena. Suprathermal streams of particles occur sporadically in such regions with sufficient density (Jefferies & Orrall 1965) to explain the observed bursts of both microwave and X-ray radiation (Acton 1966).

Variation with height.—The temperature structure of the corona with height above the chromosphere naturally divides itself into two regimes. The chromosphere-corona interface in which the temperature rises abruptly has been discussed by Pottasch (1964) and by Athay (1966) and is more appropriately examined in the review of the solar ultraviolet spectrum in this volume (Goldberg 1967). As we proceed further out into the corona, the decrease in temperature will be determined by the supply of energy from below, thermal conduction, and the loss of energy produced by the escape of material in the solar wind. We shall first summarize the observational data for the temperature of the outer corona and later examine some of the implications of this structure.

Away from active regions, temperatures in the intermediate corona may be estimated from the general gradient of coronal electron density and the width of coronal lines. Although the former technique requires the assumption of hydrostatic equilibrium, which the presence of a solar wind demonstrates to be untrue, a simple evaluation of the magnitudes of the terms in Equation 2 shows that the departures from the hydrostatic equation caused by the existence of a solar wind are insignificant in the region of subsonic expansion, i.e., below $\sim 10\ R_\odot$. The electron temperature distribution inferred

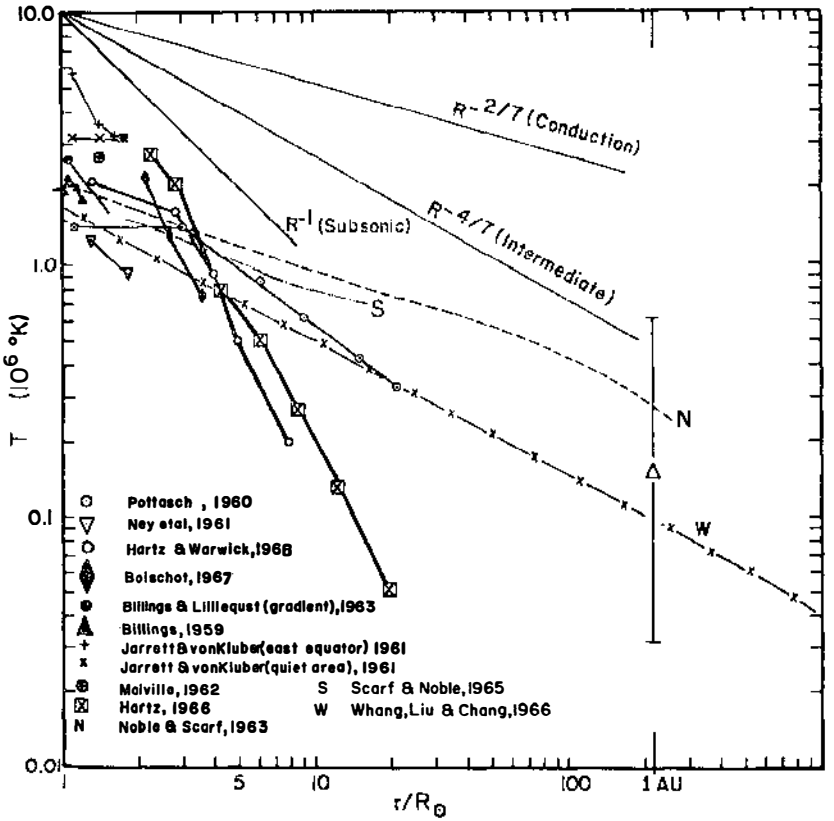

FIG. 15. The temperature structure of the solar corona. The temperature gradient in the quiet corona appears consistent with conduction from the base while that of active regions (heavy lines) appears to be so steep that only a subsonic solar wind can be maintained. Lines showing the $R^{-2/7}$, $R^{-4/7}$, and R^{-1} decay of temperature are included for comparison.

from the hydrostatic equation by Ney et al. (1961) from their observation of the 1959 eclipse and by Pottasch (1960) from a compilation of several density models thus are based on the assumption that both the influence of the solar wind and any transfer of momentum into the corona by shock waves (Kuperus 1965) are negligible (Figure 15)

Measurement of the Doppler widths of coronal emission lines allows the ion kinetic temperature and temperature gradient to be established free from any assumption of hydrostatic equilibrium although, as has already been mentioned, other uncertainties intrude. Interferometric observation of the widths of the 6370 Å and 5303 Å lines during eclipse led Jarrett & von Klüber (1961) to kinetic temperatures which even in the quiet corona exceed 3×10^6

°K. These unbelievably high values apparently result from the difficulties of determining the true Doppler profile with an interferometer whose instrumental half-width (0.6 Å) is a large fraction of the line itself. Conventional spectroscopic measurements outside of eclipse by Billings (1959), Billings & Lehman (1962), and Billings & Lilliequist (1963) yield kinetic temperatures that are consistently lower but still above those inferred from the hydrostatic equation.

The electron temperature distribution in the corona high above active regions may be discovered from the duration of type III radio bursts (Boischot, Lee & Warwick 1960, Malville 1962, Hartz & Warwick 1966, Hartz 1964 and 1966, Boischot 1967) in which a pulse of energetic particles excites oscillations in the surrounding plasma. The assumption that the oscillations are damped out by proton-electron collisions leads to a simple relation

$$T_e = 0.65 \times 10^{-4} \nu^{4/3} \tau^{2/3} \qquad 4.$$

between the electron temperature T_e, the radio (and plasma) frequency ν, and the e-folding duration τ of the burst. However, as Hughes & Harkness (1963) pointed out, the duration of a burst is actually determined both by the velocity dispersion in the spray of exciting particles and by collisional damping. Although no clear technique exists to separate these two contributions, these authors estimate, on the basis of an assumed coronal model, that only at frequencies below 100 Mc/s (above 1.5 $R_\odot$) are collisions sufficiently dominant to allow a meaningful temperature estimate.

In spite of these ambiguities type III radio bursts have several distinct advantages as a coronal thermometer. Space-probe radiometers have been able to extend these measurements down to frequencies of 0.6 Mc/s (Hartz 1966) which are taken as equivalent to a height of nearly 20 $R_\odot$. Moreover, the estimates are independent of any assumptions concerning the dynamics of the corona and may be compared directly with the theoretical models. Inspection of Figure 15 shows immediately that although the electron temperatures derived by this technique at 2–3 $R_\odot$ are roughly concordant with other measures, the indicated temperature gradients are steeper in the entire range 2.5 to 20 $R_\odot$ than either the theoretical models or the results determined from the hydrostatic equation. Remembering that the analysis of burst durations really results in a relation between temperature and density, we examine the validity of the density models chosen to establish the height scale.

First, we note that the combined observation of both frequency drift and burst position necessary for an *independent* determination of the electron density extends down to only 10 Mc/s ($\sim$4 $R_\odot$). The electron temperature estimates were made under the assumption that a particular model (e.g. 10$\times$ the Baumbach-Allen densities or 5$\times$ the background) extends out to $\sim$20 $R_\odot$ above active regions. This assumption appears unjustified; in fact, there is evidence (Michard 1954) that the enhancement of a streamer may increase at large distances to values of 20–30 times the background. We note that the perhaps more realistic assumption of a lower density gradient in the streamer

would lead to a less drastic decrease of the electron temperature above $4R_\odot$. A more consistent picture of the corona high above an active region would presumably result from a combination of the observed T vs. n_e and the dynamical equations for the solar wind.

Space-probes allow direct measurement of the energy dispersion of the interplanetary gas and show an average proton temperature of 1.5×10^5 °K but with values between 3×10^4 °K and 6×10^5 °K appearing frequently. The higher temperatures generally occur with the highest bulk velocities of the plasma (Neugebauer & Snyder 1966). One interpretation of the direction of arrival of particles at 1 a.u. is that the proton temperature transverse to the magnetic field is smaller by a factor of 5 than the longitudinal temperature (Wolfe et al. 1966) although the use of temperature to describe such an anisotropic flow is questionable. Clearly, the fact that the range of temperatures experienced in interplanetary space far exceeds that found in the lower corona indicates that the conduction model is not completely adequate.

Implications for the solar wind.—In comparing the above estimates with solar-wind models, we should remind ourselves of several conclusions regarding the relation between the temperature structure of the corona and the behavior of the wind. In the idealized isothermal solar wind the interplanetary flux, velocity, and density are all monotonically increasing (and rather sensitive) functions of the temperature T_0 at some reference level in the corona. Changes in N_0, the density at the reference level, have no other effect than to modulate the density at 1 a.u. proportionately. Parker (1965b) has shown that the role of the base density in the purely conductive corona is more critical since increasing N_0 furnishes more and more material which must be expanded and lifted out of the solar gravitational field by the limited amount of energy supplied by conduction from below. He identifies two temperature-dependent critical densities, N_A and N_B, to separate the solutions of the hydrodynamic equations into three regimes in which the flow and the temperature distribution differ vastly (Table IIIa). For $N_0<N_A$, conduction overpowers the convective loss of energy and $T\propto R^{-2/7}$ as in the purely conductive corona (Chapman 1957). At an intermediate value of N_0 the temperature drops sharply as $R^{-4/7}$ out to some radius R_2 beyond which it follows the conductive law. For $N_0>N_B$, convective losses choke off the flow of heat into the outer corona and the solar wind becomes subsonic with a fall of temperature as $\sim R^{-1}$ beyond the critical radius R_C.

In Table IIIb the values of N_A and N_B (Parker 1965b) for conditions taken to represent the quiet and active-region corona at a reference level $R=2.4\ R_\odot$ show immediately that although the quiet corona should be consistent with the purely conductive model and an approximately $R^{-2/7}$ temperature law, we might expect active regions to be described by the intermediate or even the completely subsonic cases. Comparison of the observed temperature structure with the theoretical models supports these conclusions. As well as can be determined, temperatures in the quiet corona follow that predicted by the conductive models of Noble & Scarf (1963), Scarf & Noble

TABLE III

A. CHARACTER OF THE TEMPERATURE DISTRIBUTION AND SOLAR WIND

Condition	Temperature structure	Character of solar wind at 1 a.u.
$N_0 < N_A$	$T \propto R^{-2/7}$	supersonic
$N_A < N_0 < N_B$	$T \propto R^{-4/7}$, $R \leq R_2$ $T \propto R^{-2/7}$, $R > R_2$	supersonic
$N_0 > N_B$	$T \propto R^{-4/7}$, $R \leq R_c$ $T \propto \sim R^{-1}$, $R > R_c$	subsonic

B. REPRESENTATIVE DENSITIES AT 2.4 $R_\odot$

Quiet corona	Active region
$T_0 = 1.5 \times 10^6$ °K $N_{obs} = 1.3 \times 10^6$ cm^{-3} $N_A = 10^7$ cm^{-3} $N_B = 1.2 \times 10^8$ cm^{-3}	$T_0 = 2 \times 10^6$ °K $N_{obs} = 10^7$ cm^{-3} $N_A < 10^7$ cm^{-3} $N_B = 2 \times 10^7$

(1965), or Whang, Liu & Chang (1966) quite nicely. Moreover, if we accept the approximately R^{-1} decline found from the analysis of type III burst durations, we conclude that the density is, indeed, high enough to have choked off the heat flow and that only subsonic expansion occurs in the corona above active regions. The temperature in such a "cold streamer" might be expected to decrease as $\sim R^{-1}$ to about 10^4 °K and then become constant out to the limit of the Sun's H II or Strömgren sphere at several astronomical units. At approximately the location where the temperature has dropped significantly below the conduction values (i.e., at 5–10 $R_\odot$), the density gradient would be expected to become significantly less steep than in the background corona. Although present theories are adequate for the description of isolated subsonic and supersonic winds, little attention has been given to the problem of the interaction of adjacent subsonic and supersonic sectors. The fact that space-probes always detect a substantial supersonic wind suggests that the high-speed sectors must fold in upon whatever cool sectors may exist. Since present space-probes, because of their accumulation of a net charge of a few volts, may not be capable of detecting slow particles, the existence of cool, slow streams of interplanetary plasma remains hypothetical.

Finally, we note that the assembled temperature data give scant support to the proposal that conduction is insufficient to explain the temperature structure of the inner corona and that dissipation of the energy of shock waves must extend out ot two or so solar radii (Parker 1965a). Except for the

Pottasch (1960) model there is no evidence for the broad temperature plateau which would require such a mechanism.

Magnetic Fields

Perhaps, the most central agent in determining the morphological structure of the corona is the magnetic field. The field is clearly responsible for the shape of polar plumes as well as the appearance of loops and arches in the corona above magnetically active regions on the disk. Moreover, the presence of enhanced magnetic fields in particular regions at the surface can be expected (Kulsrud 1955, de Jager 1962, Kuperus 1965) to increase the rate of transfer of mass and energy from the chromosphere into the corona. Magnetic fields must also play a vital role in moulding coronal streamers into the shapes observed and determining the distribution of mass in coronal condensations. It is rather ironic that we know so little about coronal magnetic fields. Efforts to analyze these fields have yielded information on either the configuration or the gross magnitude but rarely on both simultaneously. The detailed connection between coronal and photospheric fields has yet to be established.

Geometrical configuration.—The simplest way to examine the configuration of coronal magnetic fields is to assume that an identifiable feature such as an arch represents a magnetic tube which contains an abnormal amount of material. Thus, the arrangement of polar plumes projected against the plane of the sky may be fitted to the lines of force of an immersed dipole and the length of the dipole derived (e.g. Saito 1965a). Coronal arches visible in photographs made in the 5303 Å line appear to connect regions of opposite magnetic polarity in the photosphere with the plane of the arch perpendicular to whatever filaments may be present (Bumba, Howard & Kleczek 1965), as would be required by the theory of prominence support proposed by Kippenhahn & Schlüter (1957). A detailed polarimetric analysis of an extensive coronal condensation allowed Saito & Billings (1964) to determine the three-dimensional distribution of material and to estimate the direction of the field at various positions in the region (Figure 16). Here again the field approximately parallels the density contours, which indicates that the field is capable of containing the material.

Magnitude.—The fact that occasionally the field is of such a configuration as to support the relatively cool material of a prominence against gravity permits the conventional technique of Zeeman splitting in Hα to be used to estimate the projected magnitude and orientation of magnetic fields in coronal space (Zirin & Severny 1961). A detailed investigation of prominence fields led Rust (1966) to conclude that, indeed, prominences occur only where the field is horizontal and that the lines of force run approximately perpendicular to the long axis of a filament. The magnitudes of the fields ranged from $\sim$50 G for active-region prominences, through $\sim$15 G for prominences associated with young bipolar groups, to $\sim$5 G in the polar crown of filaments. Although the polarities of the fields found in prominences agreed with that

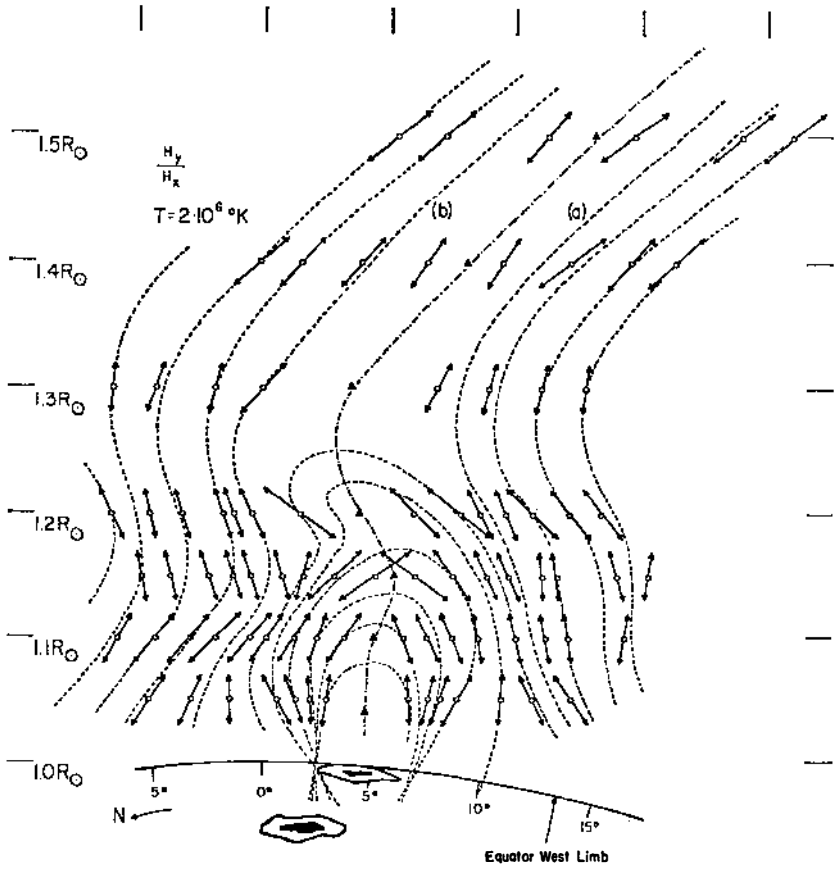

FIG. 16. The projected orientations of magnetic fields in a coronal condensation inferred from the departures of the observed density structure from hydrostatic equilibrium. (From Saito & Billings 1964.)

calculated by potential theory from the underlying photospheric fields, Rust discovered that the observed magnitudes were far in excess of those calculated. Whether this discrepancy is due to the neglect of weak photospheric fields outside the region considered to be the source, or to the increase of the coronal field strength by twisting is unknown.

Measurement of the polarization of emission lines is also capable of yielding estimates of the magnetic field since the plane and magnitude of polarization are governed by competition between resonance scattering of photospheric light and the perturbation of the atomic energy levels by the field (Warwick & Hyder 1965, Hyder 1965b). Field strengths determined from polarimetry of prominence lines (Brückner 1963, Hyder 1964, 1965c) appear in agreement with the corresponding Zeeman estimates. The magnetic per-

turbation for forbidden lines such as 5303 Å is so great that studies of their polarization (Charvin 1964, Hyder 1965c, Eddy & Malville 1966) have been unable to yield data on coronal magnetic fields.

A unique estimate of the magnetic field in a filament and the surrounding corona has been made by Hyder (1966b) from the decay of the oscillatory motion of a winking filament. The frequency of the oscillation required a field in the range 2–30 G in the prominences while the viscosity needed to produce the observed damping suggested fields greater than 0.1–0.2 G in the surrounding corona. It is of interest that all these estimates give fields in prominences much smaller than those required by Warwick (1957) to account for the observed curvature in the trajectories of flare-associated spray prominences. Apparently the sprays represent events in which the ejected material stretches abnormally intense fields high into coronal space. Under the bold assumption that all these estimates of prominence magnetic fields are roughly appropriate to the corona, we place them in Figure 17, in which the field magnitude is plotted against height above the surface.

The propagation of radio waves through the coronal plasma is profoundly influenced by the presence of a magnetic field. Not only is the opacity increased by the mechanism of magnetoionic resonance (Zhelezniakov 1962, Kundu 1965) but also the refractive index and opacity become dependent upon the polarization and direction of propagation. Since the height in the corona corresponding to optical depth unity is then different for extraordinary and ordinary modes of propagation, the resultant thermal radiation from coronal condensations and active-region enhancements is polarized. Following earlier investigators (Gelfreich et al. 1958, Christiansen et al. 1960, Korol'kov & Soboleva 1962), Kakinuma & Swarup (1962) have used the observed variation of polarization of the slowly varying component with frequency and position of the region on the disk to derive a self-consistent model of the magnetic field above active regions. Although the method requires the assumption of a rather idealized configuration of the field in order to be mathematically tractable, it appears to be the least uncertain of all the techniques for estimating coronal magnetism.

The characteristics of radio bursts also permit the estimation of coronal magnetic fields, although the relatively straightforward observations are often subject to a variety of interpretations. For example, the sense of circular polarization of microwave bursts is found to reverse at a frequency of $\sim 4 \times 10^3$ Mc/s and the profile of emitted flux about the reversal frequency is remarkably similar from burst to burst. Takakura (1960) attributes the microwave bursts to synchrotron radiation and the reversal of polarization to resonance absorption in the extraordinary mode at the gyrofrequency in the source region. Conversely, Cohen (1961) takes the site of the anomalous absorption and the polarization reversal to be at a location where the field is approximately perpendicular to the escaping radiation at an altitude of some 10^5 km. Thus, the basic datum appears to be explained by either a field of ~ 600 G at 3×10^4 km or one of ~ 4 G at 10^5 km.

The interpretation of other radio-burst phenomena is subject to similar

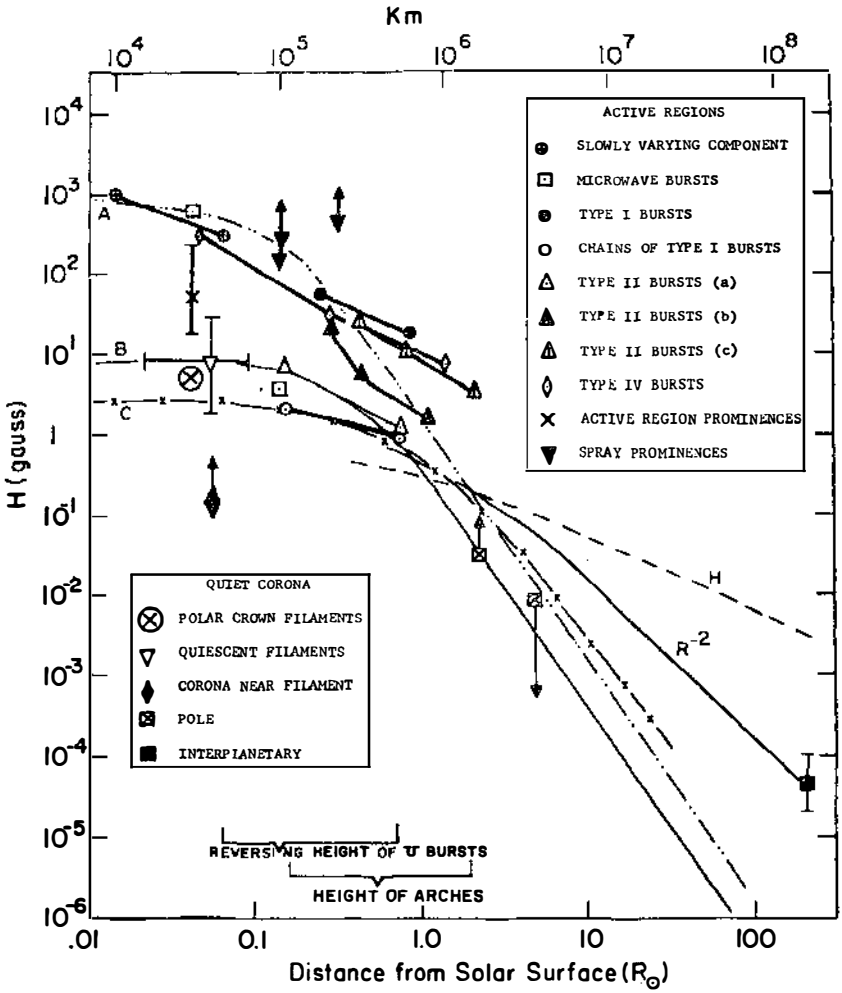

FIG. 17. The strength of coronal magnetic fields as a function of height above the photosphere as estimated by various techniques. Values referring to active regions appear as heavy lines. Simple models for the potential field above an active region (*A*), an extended dipole region (*B*), and the general solar field at the equator (*C*) appear for comparison. The curve *H* represents the field required for pressure equilibrium with the solar wind.

uncertainties. Takakura (1966) regards type I bursts as the result of coherent plasma oscillations excited by electrons traveling at a few times the mean thermal speed. The upper limit of field required to accelerate these electrons by the Fermi mechanism and the lower limit needed to explain their polariza-

tion establish the field strength at a few tens of gauss in the frequency range 50–200 Mc/s (height range 10^5 to 2×10^6 km). Examination of chains of type I bursts, on the other hand, led Wild & Tlamicha (1965) to conclude that the field strengths are at least an order of magnitude lower. They make no assumption concerning the details of the excitation of the bursts but interpret the frequency drift observed in a chain as an upward-propagating Alfvén wave.

Type II bursts have given rise to no less than three rather distinct estimates of coronal magnetic fields. From their time-frequency behavior and the assumption that the burst exciter is a hydromagnetic shock wave (Takakura 1966, Fomichev & Chertok 1966), it is possible to set limits for the field at a given frequency or height [type II bursts (*a*), Figure 17]. Field strengths may also be inferred from the splitting of these bursts although there appears to be no unanimity as to just how the data are to be interpreted. Considered as a magnetoionic phenomenon similar to the Zeeman effect, the observed splittings (Maxwell & Thompson 1962, Takakura 1966) lead to values somewhat in excess of the limits imposed by the shock-wave model [type II bursts (*b*), Figure 17]. However, as pointed out by Weiss (1965), there is even some question whether the splitting should be considered a true magnetoionic effect with a splitting half the gyrofrequency, or a simple beat phenomenon, with a splitting equal to the gyrofrequency. Other models of the splitting formulated by Sturrock (1961), in which two exciter waves propagate at different angle to the magnetic field, and by Tidman, Birmingham & Stainer (1966), in which the exciter is a cluster of electrons with an anisotropic velocity distribution, require still higher values of the field [type II bursts (*c*), Figure 17]. Even the basic premise that the splitting is due to the magnetic field has been questioned by Roberts (1959), who points out that the plausible formation of a double front in the exciting shock wave could also explain the observations.

The analysis of type III bursts, believed to be excited by a pulse of relativistic particles, has yielded still less information on coronal magnetic fields. The fact that some bursts are polarized while others appear unpolarized allows the field strength to be estimated only between limits of nearly two orders of magnitude.

The frequency distribution of the radiation of type IV bursts can give an idea of the field since the maximum flux is expected at twice the gyrofrequency. However, resonance absorption at the gyrofrequency and its harmonics will shift the maximum by an uncertain amount; and the fields recorded in Figure 17 for type IV bursts were derived by Takakura (1966) under the assumption that the maximum occurs at 4 times the gyrofrequency. It is quite clear that the majority of estimates of coronal magnetic fields in the height range 10^5 to 10^6 km from radio bursts all suffer from a common difficulty—the unknown validity of the assumed excitation mechanism. An order-of-magnitude uncertainty in the field strength results.

Beyond one solar radius from the surface only limits are available for

coronal magnetic fields. Högbom's (1960) earlier mentioned study of coronal irregularities suggested that polar plumes are maintained out to at least 3 $R_\odot$. Using a standard model for polar densities, he thus concluded that a field of at least 3×10^{-2} G was required to contain the plumes against lateral expansion at that height An upper limit to the field of 8×10^{-3} G at 5–6 $R_\odot$ was found by Golnev, Parijstky & Soboleva (1964) from the absence of any detectable Faraday rotation in the radiation from the Crab Nebula as it was occulted by the corona

The measurement of interplanetary magnetic fields has been discussed in an earlier section and reviewed in detail elsewhere in this volume (Ness 1967). For comparison with the other estimates in Figures 17 we note that the magnitude of the field varies between 2×10^{-5} G and 10^{-4} G with an average of about 5×10^{-5} G (Greenstadt 1966). The direction of the field is generally along the Archimedes spiral (Ness, Scearce & Seek 1963) although wide variations in direction show that the field is often kinked and twisted (McCracken & Ness 1966). The close connection of the direction of the interplanetary field and that present on the Sun demonstrated by Wilcox & Ness (1965) suggests that the solar fields are indeed swept into space by the solar wind.

Interaction of the magnetic field and the solar wind.—In the attempt to integrate the various measures of coronal magnetic fields, we have added several simple calculations to Figure 17. Curves *A*, *B*, and *C* represent the decrease in field strength above the equator of simple dipoles taken to represent an active region, an extended magnetic-dipole region such as visualized by Leighton (1964), and the general magnetic field of the Sun, respectively. The parameters of these oversimplified models appear in Table IV. Two other curves show the R^{-2} dependence fitted to the interplanetary value and *H*, the field necessary to give a magnetic pressure just equal to the dynamic pressure of the solar wind taken from the isothermal model with $T_0=2\times10^6$ °K. Although no particular merit is claimed for these calculations, they suggest the following conclusions. First, the potential dipole model appears capable of yielding at least a crude representation of the magnetic field above active regions and the more quiet portions of the Sun. Second, comparison of these fields with the curve *H* implies that below a

TABLE IV

PARAMETERS OF THE POTENTIAL FIELD MODELS

Model	Flux at surface (maxwells)	Separation between poles
A (active region)	3×10^{22}	2×10^4 km
B (extended dipole)	3×10^{21}	3×10^5 km
C (general)	3×10^{22}	5×10^5 km (0.7 $R_\odot$)

height of $\sim 3\ R_\odot$ the coronal material is controlled by the magnetic field. It is equally clear that above this height the coronal magnetic fields are being strung out into interplanetary space by the solar wind. This conclusion is supported by the observation that the highest closed arches visible in the eclipse data assembled by Bugoslavskaya from 1887 to 1945 have a mean height of only $0.6\ R_\odot$ above the limb and that the maximum height of U bursts is some 4×10^5 km ($0.57\ R_\odot$) (Takakura 1966). The fact that the R^{-2} curve intersects the others in the same region implies that the measured interplanetary fields are simply those which have been unraveled from the corona at this level. Finally we note that the dominance of the solar wind above $\sim 3\ R_\odot$ precludes rigid rotation of the corona with the Sun further out into the solar system.

The detailed theoretical investigation of the interaction of the solar wind and coronal magnetic fields is one of great complexity. A complete solution of the problem would have as its boundary conditions the distribution of magnetic fields as well as the variation of flux into the corona from place to place on the surface. The flow of the material will, of course, distort the field and conversely the presence of the field will modify the flow. The resultant distribution of material should then be that of the corona we see with its streamers and other features. Parker (1958) has described the basic pattern of the dipole field extended by the solar wind while both he (Parker 1963) and Pneuman (1966a, b) have attempted to estimate the detailed density distribution and field configuration near the Sun. Parker reasoned that the escape of the solar wind must be primarily at the equator and formally calculated the configuration of the field with a conducting sheet interposed at the equator. Material flowing out along the lines of force produces a distribution of density reminiscent of an equatorial coronal streamer (Figure 18). Pneuman divided the flow into two regimes in which the stream lines follow the dipole field close to the Sun and are radial far out, but was unable to calculate their form in the crucial intermediate region (Figure 19).

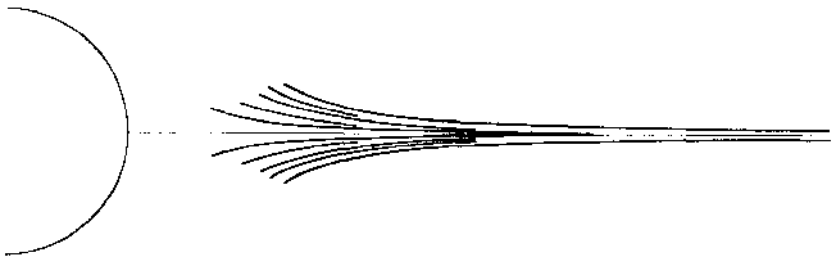

FIG. 18. Contours of equal density in the corona are distorted into a "streamer" by the presence of a dipole field in the solar wind. This calulated structure, although made for a flow model slightly different from that shown in Figure 19, demonstrates that the apparent shape of a streamer cannot be taken as representing the flow lines of the material. (From Parker 1963.)

One consequence of the magnetic field is to reduce the velocity of the solar wind at the equator compared to that at high latitudes. Comparison of Figures 18 and 19 shows rather dramatically that the apparent shape of a coronal streamer can no-wise be equated with the flow lines of the material

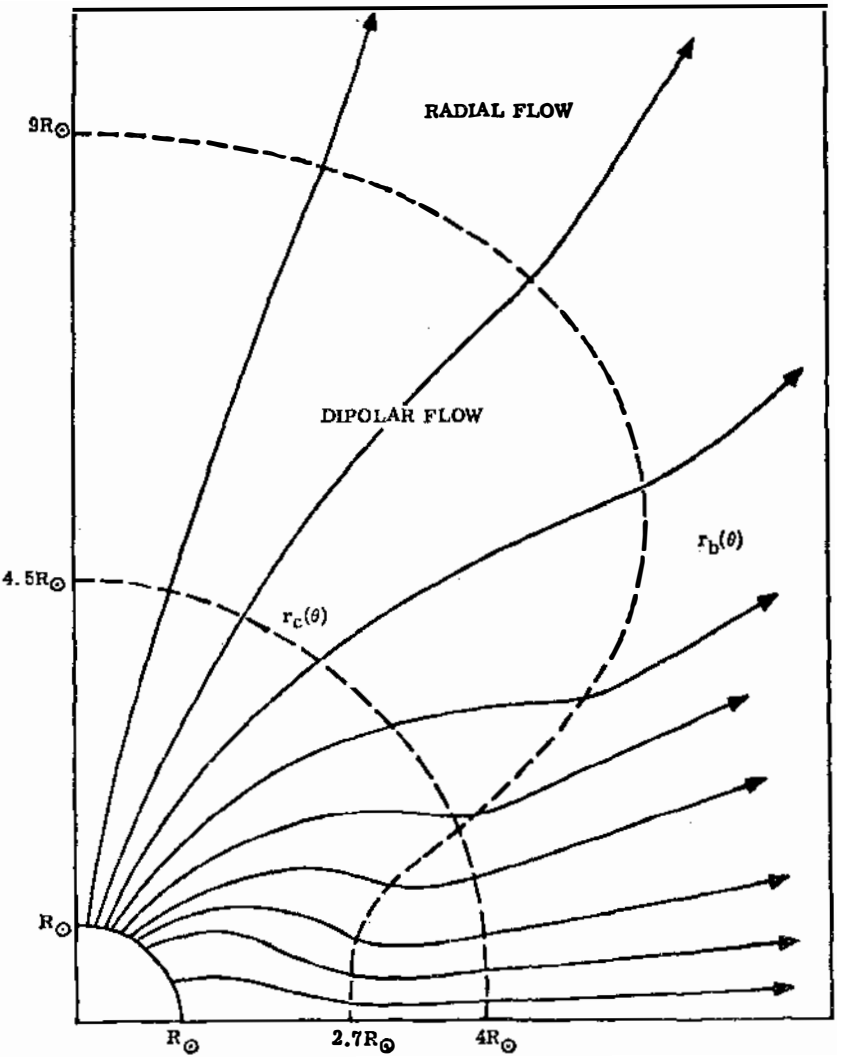

FIG. 19. Stream lines in the solar wind are distorted toward the equator by the presence of the general, dipole magnetic field during sunspot minimum. The velocity of the wind is also modified so that the equatorial speeds are slower than those at the pole. (From Pneuman 1966a.)

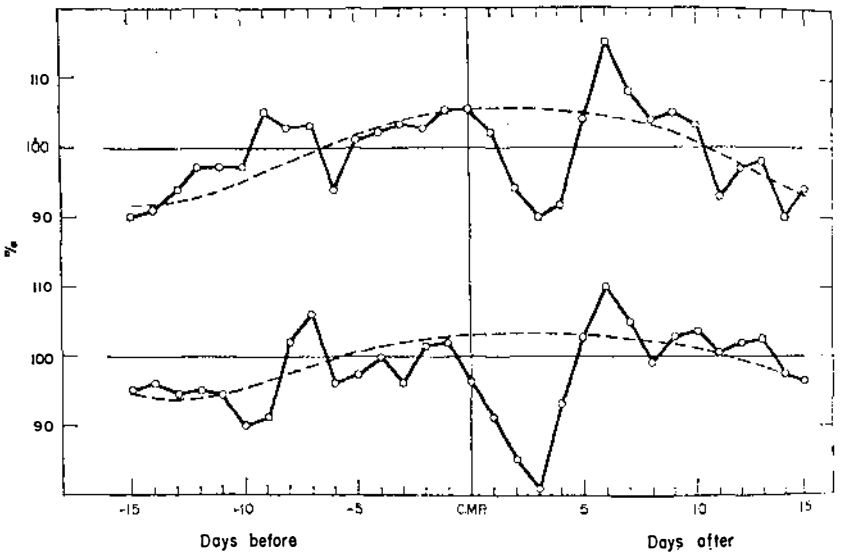

FIG. 20. The superposed variation of the geomagnetic character figure K_p with respect to the central meridian passage of plages. Only recurrent or M-region magnetic storms are considered. The top graph contains data for the brightest plages occurring at all phases of the sunspot cycle while the lower one considers only the declining portion of the cycle. (From C. W. Allen 1964.)

except far from the Sun where radial, supersonic expansion obtains. Although calculations of the interaction of the solar wind with the more complex fields in active regions or in the neighborhood of filaments have not been attempted, we can be confident that a similar distortion of the flow and a "coronal streamer" will result.

THE CORONA AND GEOMAGNETIC ACTIVITY

The basic question "What is the connection between visible forms in the corona and geomagnetic activity?" still has no uniformly accepted and satisfactory answer. Since geomagnetic storms are one of the most spectacular features of geomagnetism, many of the early investigations (see the reviews of Chapman & Bartels 1940, Mustel' 1964, Allen 1964) attempted to relate the occurrence of storms to particular solar surface features. These statistical studies were handicapped in several ways. First, as a detector of the state of the interplanetary medium, the geomagnetic field at the surface is unsatisfactory since it is uncertain whether the "storm" is caused by an increase in the interplanetary density, velocity, flux, energy density, magnetic field, or in the time fluctuation of these parameters. [Recent space-probe measurements suggest that the K_P index is controlled by the velocity of the interplanetary stream (Neugebauer & Snyder 1966) although it appears that

the intensity of the magnetic field is also an important factor (Wilcox, Schatten & Ness 1966)]. Second, both the source on the Sun and the velocity of particles were unknown and had to be inferred from the statistical data. Third, synoptic observations of the intermediate and outer corona were, and still are, unavailable so that the connection of, for example, geomagnetic storms with streamers had to be inferred from the correlation of both of these with an intermediate feature such as prominences.

These statistical studies frequently divide geomagnetic disturbances into large storms, which occur around and immediately following sunspot maximum, and moderate and small storms, which continue to be found through the declining portion of the solar cycle into minimum. The large storms seldom recur for more than one or two solar rotations while the small storms may reappear at 27-day intervals for many months or even years. It was early recognized that nonrecurrent storms follow the passage of active regions across the disk by ~3 days, and the natural conclusion was drawn that the region was the source of particles streaming outward from the Sun at a speed of ~600 km/s. [Impulsive disturbances in the geomagnetic field following solar flares are attributed to blast waves (Parker 1963) in the corona and are not directly associated with any permanent solar feature.] No such simple conclusion could be reached for the recurrent storms, which show a minimum in K_P ~3 days after the central meridian passage (CMP) of an active region and a maximum ~6 days after CMP (Figure 20). The lack of any obvious candidate for the source of these storms has led to the hypothesis of the "M region" which has been variously, and not very successfully, identified with plages, the space between plages, prominences, unipolar magnetic regions, and streamers (Allen 1964).

Two schools of thought have developed around the controversy of whether the maximum or the minimum is the principal event. The "cone of avoidance" school regards the minimum at CMP+3 days as evidence for a vacancy (Pecker & Roberts 1955) above the active region caused by the magnetic steering of particles toward the boundary of the region. A later modification of this picture (Billings & Roberts 1964) suggests that the material immediately over the region is contained by the magnetic field while that at the border is allowed to escape as the solar wind. The presence of the minimum at CMP+3 days with regions bright in the 5303 Å line (Bell & Glaser 1957) rather than active regions appears to support this idea. Outside the "cone of avoidance" the solar wind is considered to have a speed of ~600 km/s. The "*R*-ray" school, championed for many years by Mustel' (1961, 1962a, 1962b, 1964), considers the minimum of completely secondary importance and the maximum at CMP+6 days as evidence for the arrival of particles at a speed of ~300 km/s from the center of the active region. Support for this theory is claimed from the fact that active regions appear to have high coronal densities extending far out into the corona.

Unfortunately, the advent of space-probes from which the speed of the interplanetary particles may be measured has done little to resolve the

dilemma. Using the plasma velocities found by Mariner II, Snyder & Neugebauer (1966) attempted to locate the sources of several well-defined magnetic storms and could find no consistent connection of the storms with either active-region plages or, as the "cone of avoidance" hypothesis would dictate, the interplage areas. The satellite observations also show (Wilcox & Ness 1965) that the structure of the solar wind within a given sector is extremely complex. Particles with the highest speeds at 1 a.u. do not, as would be suggested by Mustel"s (1964) models, arrive at the beginning of the sector but several days later.

Returning to the corona, we note that streamers are known to occur over active regions, over prominences, and occasionally over areas which have no distinctive appearance whatsoever (Bohlin, Hansen & Newkirk 1966). Both from our earlier discussion of the temperature profile over active regions and from Pneuman's (1966a) study of the solar wind above the equator of a dipole, we should expect that the solar wind from active regions shoud be reduced or completely choked off to create a "cone of avoidance" in the *flux*. The lower field intensities and density in streamers over prominence would suggest that such features could be a likely source of geomagnetic storm particles. However, Dizer (1963) finds no correlation of geomagnetic activity over the period 1920–1954 with long-lived filaments. Mustel' (1964) interprets this as evidence that such streamers do not penetrate more than ~ 30 $R_\odot$ into the solar system although an equally satisfactory explanation is that their generally high latitude causes them to miss the Earth. Certainly, there is much reason to believe that there are large variations in the speed of the solar wind from place to place on the Sun. How these variations compare with visible structures in the corona and how streams of different velocity interact in interplanetary space to produce the wind observed at the orbit of Earth is presently unknown.

LITERATURE CITED

Acton, L. W. 1966, *Ap. J.* (Submitted August 1966)

Allen, C. W. 1963a, *Astrophysical Quantities* (2nd ed., Athlone Press, London)

Allen, C. W. 1963b, in *The Solar Corona, IAU Symp. No.* **16** (Academic Press, New York)

Allen, C. W. 1964, *Planetary Space Sci.*, **12**, 487–94

Antrack, D., Biermann, L., Lüst, R. 1964, *Ann. Rev. Astron. Ap.*, **2**, 327

Athay, R. G. 1966, *Ap. J.*, **146**, 223

Axford, W. I., Dessler, A. J. Gottlieb, B. 1963, *Ap. J.*, **137**, 1268

d'Azambuja, M., d'Azambuja, L. 1948, *Ann. Obs. Paris*, **6**

Babcock, H. W. 1961, *Ap. J.*, **133**, 572

Bartley, W. C., Bukata, R. P., McCracken, K. G., Rao, U. R. 1966, *J. Geophys. Res.*, **71**, 3297

Bell, B., Glaser, H. 1957, *Smithsonian Contrib. Ap.*, **2**, 51

Biermann, L. 1951, *Z. Ap.*, **29**, 274

Biermann, L. 1957, *Observatory*, **107**, 109

Biermann, L., Lüst, R. 1966, in *The Solar Wind*, 3–23 (Jet Propulsion Lab. and California Inst. of Technol., Pasadena)

Billings, D. E. 1959a, *Ap. J.*, **130**, 215–20

Billings, D. E. 1959b, *Solar Res. Memo No. 137* (28 December)

Billings, D. E. 1965, *Ap. J.*, **141**, 325

Billings, D. E. 1966, *A Guide to the Solar Corona* (1st ed., Academic Press, New York)

Billings, D. E., Lehman, R. C. 1962, *Ap. J.*, **136**, 258–65

Billings, D. E., Lilliequist, C. G. 1963, *Ap. J.*, **137**, 16

Billings, D. E., Roberts, W. O. 1964, *Astron. Norveg.*, **9**, 147–50

Blackwell, D. E., Ingham, M. F. 1961, *Monthly Notices Roy. Astron. Soc.*, **122**, 129

Bohlin, J. D., Hansen, R. T., Newkirk, G. A. 1966 (Paper presented at October meeting A.A.S.)

Boischot, A. 1967, *Ann. Ap.*, **30**, 85

Boischot, A., Lee, R. H., Warwick, J. W. 1960, *Ap. J.*, **131**, 61–67

Brandt, J. C. 1964, *Science*, **146**, 1671

Brandt, J. C. 1966, *Ap. J.*, **144**, 1221

Brandt, J. C., Belton, M. J. S., Stevens, M. W. 1966, *Astron. J.*, **71**, 157

Brückner, G. 1963, *Z. Ap.*, **58**, 73

Bugoslavskaya, E. Y. 1949, *Publ. Sternberg Inst.*, **19**

Bumba, V., Howard, R., Kleczek, J. 1965, *Publ. Astron. Soc. Pacific*, **77**, 55

Burgess, A. 1964, *Ap. J.*, **139**, 776

Burgess, A. 1965, *IAU Symp. No. 23*, 95–99

Chamberlain, J. W. 1960, *Ap. J.*, **131**, 47

Chamberlain, J. W. 1961, *ibid.*, **133**, 675

Chapman, S. 1957, *Smithson. Contrib. Ap.*, **2**, 1

Chapman, S., Bartels, J. 1940, *Geomagnetism* (Oxford Univ. Press, New York)

Charvin, P. 1964, *Compt. Rend.*, **259**, 733

Chisholm, J. H., James, J. C. 1964, *Ap. J.*, **140**, 377–79

Christiansen, W. N., Mathewson, D. S., Pawsy, J. L., Smerd, S. F., Boischot, A., Denisse, J. F., Simon, P., Kakinuma, T., Dodson-Prince, H., Firor, J. 1960, *Ann. Ap.*, **23**, 75

Cohen, M. H. 1961, *Ap. J.*, **133**, 978

Cohen, M. H., Gundermann, E. J., Hardebeck, H. E., Harris, D. E., Salpeter, E. E., Sharp, L. E. 1966, *Science*, **153**, 745

Coleman, P. J., Davis, L., Smith, E. J., Sonett, C. P. 1962, *Science*, **138**, 1100

Cooper, R. H., Billings, D. E. 1962, *Z. Ap.*, **55**, 24–28

Deutsch, A. J., Righini, G. 1964, *Ap. J.*, **140**, 313

Dizer, M. 1963, *Observatory*, **82**, 250

Dollfus, A. 1957, *Compt. Rend.*, **244**, 1880–83

Dollfus, A. 1958, *ibid.*, **246**, 2345

Eddy, J. A., Malville, J. M. 1966 (Paper presented at October meeting A.A.S.)

Erickson, W. C. 1964, *Ap. J.*, **139**, 1290–1311

Evans, J. W. 1957, *Publ. Astron. Soc. Pacific*, **69**, 421

Evans, J. W., Michard, R., Servajean, R. 1963, *Ann. Ap.*, **26**, 368

Fan, C. Y., Lamport, J. E., Simpson, J. A., Smith, D. R. 1966, *J. Geophys. Res.*, **71**, 3289

Fokker, A. D. 1965, *Bull. Astron. Inst. Neth.*, **18**, 111–24

Fomichev, V. V., Chertok, J. M. 1966, *Soviet Astron.*, **9**, 976

Gelfreich, G., Korol'kov, D., Rishkov, N., Soboleva, N. 1958, *Paris Symp. Radio Astron.*, 125–28

Giese, R. H. 1961, *Z. Ap.*, **51**, 119

Gillett, F. C., Stein, W. A., Ney, E. P. 1964, *Ap. J.*, **140**, 292–305

Ginzburg, V. L., Zhelezniakov, V. V. 1958, *Soviet Astron.—AJ*, **2**, 653

Godoli, G. 1965, in *Stellar and Solar Magnetic Fields*, 149 (Lüst R., Ed., North-Holland, Amsterdam)

Gold, F. 1959, *J. Geophys. Res.*, **64**, 1665

Goldberg, L. 1967, *Ann. Rev. Astron. Ap.*, **5**
Golnev, V. J., Parijstky, Y. N., Soboleva, N. S. 1964, *Izv. Glavnoi Astron. Obs.*, **23**, 22–24
Greenstadt, E. W. 1966, *Ap. J.*, **145**, 270–95
Hansen, R. T., Hansen, S. 1966 (Privately circulated manuscript)
Hartz, T. R. 1964, *Ann. Ap.*, **27**, 831
Hartz, T. R. 1966 (Privately circulated manuscript)
Hartz, T. R., Warwick, J. W. 1966 (Privately circulated manuscript)
Harvey, J. W. 1965, *Ap. J.*, **141**, 832–34
Hata, S., Saito, K. 1966, *Ann. Tokyo Astron. Obs., 2nd Ser.*, **10**, 16
Hepburn, N. 1955, *Ap. J.*, **122**, 445–59
Hewish, A. 1955, *Proc. Roy. Soc. A*, **228**, 238
Hewish, A. 1958, *Monthly Notices Roy. Astron. Soc.*, **118**, 534
Hewish, A., Scott, P. F., Wills, D. 1964, *Nature*, **203**, 1214–17
Hewish, A., Wyndham, J. D. 1963, *Monthly Notices Roy. Astron. Soc.*, **126**, 469
Högbom, J. A. 1960, *Monthly Notices Roy. Astron. Soc.*, **120**, 530
Howard, R. 1959, *Ap. J.*, **130**, 193
Hughes, M. P., Harkness, R. L. 1963, *Ap. J.*, **138**, 239
Hulst, H. C. van de. 1950a, *Bull. Astron. Inst. Neth.*, **11**, 135–50
Hulst, H. C. van de. 1950b, *ibid.*, 150–60
Hulst, H. C. van de. 1953, in *The Sun* (Univ. of Chicago Press)
Hyder, C. L. 1964, *Ap. J.*, **140**, 817
Hyder, C. L. 1965a, *Ap. J.*, **141**, 272
Hyder, C. L. 1965b, *Ap. J.*, **141**, 1374
Hyder, C. L. 1965c, *ibid.*, 1382
Hyder, C. L. 1966a, *ibid.*, **146**, 748
Hyder, C. L. 1966b, *Z. Ap.*, **63**, 78–84
Jager, C. de. 1962, *Space Sci. Rev.*, **1**, 487–521
James, J. C. 1966, *Ap. J.*, **146**, 356
Jarrett, A. H., Klüber, H. von. 1961, *Monthly Notices Roy. Astron. Soc.*, **122**, 223
Jefferies, J. T., Orrall, F. Q. 1965, *Ap. J.*, **141**, 505
Kakinuma, T., Swarup, G. 1962, *Ap. J.*, **136**, 975–94
Karimov, M. G. 1961, *IAU Symp. No. 16*, 297–300
Kawabata, K. 1963, in *The Solar Corona*, 143 (Academic Press, New York)
Kellogg, P. J., Ney, E. P. 1959, *Nature*, **183**, 1297
Kiepenheuer, K. O. 1953, in *The Sun* (Univ. of Chicago Press)
Kippenhahn, R., Schlüter, A. 1957, *Z. Ap.*, **43**, 36
Kleczek, J. 1963, *Publ. Astron. Soc. Pacific*, **75**, 9–14
Korol'kov, D. V., Soboleva, N. S. 1962, *Soviet Astron.—AJ*, **5**, 491
Kulsrud, R. M. 1955, *Ap. J.*, **121**, 461
Kundu, M. R. 1965, *Solar Radio Astronomy* (Interscience, New York)
Kuperus, M. 1965, *Rech. Astron. Obs. Urecht*, **17**(1), 1–69
Leighton, R. B. 1964, *Ap. J.*, **140**, 1547
LeSqueren-Malinge, A. M. 1964, *Ann. Ap.* **27**, 183
Lilliequist, C. G. 1966 (Paper presented at October meeting A.A.S.)
Lüst, R. 1962, *Space Sci. Rev.*, **1**, 522–52
Lüst, R., Schlüter, A. 1955, *Z. Ap.*, **38**, 190
Lyot, B. 1944, *Ann. Ap.*, **1**, 41–44
McCraken, K. G., Ness, N. F. 1966, *J. Geophys. Res.*, **71**, 13
Malitson, H. H., Erickson, W. C. 1966, *Ap. J.*, **144**, 337–51
Malville, J. M. 1962, *Ap. J.*, **136**, 266–75
Mandelshtam, S. L. 1964, *IAU Symp. No. 23*, 81–89
Maxwell, A. 1965, in *The Solar Spectrum*, 342–97 (Reidel Publ. Co., Dordrecht)
Maxwell, A., Thompson, A. R. 1962, *Ap. J.*, **135**, 138–50
Meyer, F., Schmidt, H. 1966, *Mitt. Astron. Ges.*, **21**
Michard, R. 1954, *Ann. Ap.*, **17**, 429
Morimoto, M. 1964, *Publ. Astron. Soc. Pacific* **16**, 163–69
Müller, R. 1954, *Z Ap.*, **35**, 61
Mustel', E. R. 1961, *IAU Symp. No. 16* (Academic Press, New York)
Mustel', E. R. 1962a, *Astron. Zh.*, **39**, 418
Mustel', E. R. 1962b, *ibid.*, 619
Mustel', E. R. 1964, *Space Sci. Rev.*, **3**, 139–231
Ness, N. F. 1968, *Ann. Rev. Astron. Ap.* (To be published)
Ness, N. F., Scearce, C. S., Cantarano, S. 1966, *J. Geophys. Res.*, **71**, 3305
Ness, N. F., Scearce, C. S., Seek, J. B. 1963, *J. Geophys. Res.*, **69**, 3531
Neugebauer, M., Snyder, C. W. 1966, in *Solar Wind*, 3–23 (Jet Propulsion Lab. and California Inst. of Technol., Pasadena)
Newkirk, G. A. 1957, *Ann Ap.*, **20**, 127–36
Newkirk, G. A. 1961, *Ap. J.*, **133**, 983–1013
Newkirk, G. A., Bohlin, J. D. 1963, *Appl. Opt.*, **2**, 131
Newkirk, G. A., Bohlin, J. D., 1964, *ibid.*, **3**, 543
Newkirk, G. A., Bohlin, J. D. 1965, *Ann. Ap.*, **28**, 234
Ney, E. P., Huch, W. F., Kellogg, P. J., Stein, W., Gillett, F. 1961, *Ap. J.*, **133**, 616

Noble, L. M., Scarf, F. L. 1963, *Ap. J.*, **138**, 1169
Noxon, J. F. 1966, *Ap. J.*, **145**, 400–10
Oster, L., Sofia, S. 1965, *Ap. J.* **141**, 1139
Parker, E. N. 1958, *Ap. J.*, **128**, 664
Parker, E. N. 1963, *Interplanetary Dynamical Processes* (Interscience, New York)
Parker, E. N. 1964, *Ap. J.*, **139**, 690
Parker, E. N. 1965a, *Space Sci. Rev.*, **4**, 666–708
Parker, E. N. 1965b, *Ap. J.*, **141**, 1463–78
Pecker, J.-C., Roberts, W. O. 1955, *J. Geophys. Res.*, **60**, 33
Pneuman, G. W. 1966a, *Ap. J.*, **145**, 242–54
Pneuman, G. W. 1966b, *ibid.*, 800
Pottasch, S. R. 1960, *Ap. J.*, **131**, 68–74
Pottasch, S. R. 1964, *Space Sci. Rev.*, **3**, 816
Roberts, J. A. 1959, *Australian J. Phys.*, **12**, 327
Rust, D. M. 1966, *Measurements of the Magnetic Fields in Quiescent Solar Prominences* (Thesis, Univ. of Colorado, Boulder, Colo.)
Saito, K. 1958, *Publ. Astron. Soc. Japan*, **10**, 49
Saito, K. 1959, *ibid.*, **11**, 234–52
Saito, K. 1965a, *ibid.*, **17**, 1
Saito, K. 1965b, *ibid.*, **17**, 421
Saito, K., Billings, D. E. 1964, *Ap. J.*, **140**, 760
Scarf, F. L., Noble, L. M. 1965, *Ap. J.*, **141**, 1479
Schmidt, M. 1953, *Bull. Astron. Soc. Neth.*, **12**, 61–67
Seaton, M. J. 1962, *Observatory*, **82**, 111
Severny, A. B. 1965, *Soviet Astron.*, **9**, 171
Sheeley, N. R. 1964, *Ap. J.*, **140**, 731
Shklovsky, I. S. 1965, in *Physics of the Solar Corona* (2nd ed., Pergamon Press, New York)
Simon, G. W., Leighton, R. B. 1964, *Ap. J.*, **140**, 1120
Slee, O. B. 1961, *Monthly Notices Roy. Astron. Soc.*, **123**, 223
Slee, O. B. 1966, *Planetary Space Sci.*, **14**, 255–67
Slee, O. B., Higgins, C. S. 1966, *Australian J. Phys.*, **19**, 167–80
Snyder, C. W., Neugebauer, M. 1966, in *The Solar Wind*, 25 (Jet Propulsion Lab. and California Inst. of Technol., Pasadena)
Sturrock, P. A. 1961, *Nature*, **192**, 58
Takakura, T. 1960, *Publ. Astron. Soc. Japan*, **12**, 325
Takakura, T. 1966, *Space Sci. Rev.*, **5**, 80
Tidman, D. A., Birmingham, T. J., Stainer, H. M. 1966, *Ap. J.*, **146**, 207
Trellis, M. 1957, *Suppl. Ann. Ap.*, **5**
Vitkevitch, V. V. 1961, *Soviet Astron.*, **4**, 897
Vitkevitch, V. V., Antonova, T. D., Vlasov, V. I. 1966, *Soviet Phys. "Doklady,"* **11**, 369
Waldmeier, M. 1947, *Astron. Mitt. Zurich, No. 151*
Waldmeier, M. 1950, *Z. Ap.*, **21**, 24
Waldmeier, M. 1955, *ibid.*, **38**, 37
Waldmeier, M. 1957, *Die Sonnenkorona II* (Birkhauser Verlag, Basel)
Waldmeier, M. 1963, in *The Solar Corona*, 129 (Academic Press, New York)
Waldmeier, M., Müller, H. 1950, *Z. Ap.*, **27**, 58
Warwick, J. W. 1957, *Ap. J.*, **125**, 811
Warwick, J. W. 1965, in *Solar System Radio Astronomy*, 131–70 (Plenum Press, New York)
Warwick, J. W., Hyder, C. L. 1965, *Ap. J.*, **141**, 1362
Weinberg, J. L. 1964, *Ann. Ap.*, **27**, 718
Weiss, A. A. 1965, *Australian J. Phys.*, **18**, 167
Weiss, A. A., Sheridan, K. V. 1962, *J. Phys. Soc. Japan*, **17**, *Suppl. A-II*, 223
Whang, Y. C., Liu, C. K., Chang, C. C. 1966, *Ap. J.*, **145**, 255
Widing, K. G. 1966, *Ap. J.*, **145**, 380–99
Wilcox, J. M., Ness, N. F. 1965, *J. Geophys. Res.*, **70**, 5793
Wilcox, J. M., Schatten, K. H., Ness, N. F. 1966, *Space Science Laboratory Report, Ser. 7*, No. 29
Wild, J. P., Sheridan, K. V., Neylan, A. A. 1959, *Australian J. Phys.*, **12**, 369
Wild, J. P., Smerd, S. F., Weiss, A. A. 1963, *Ann. Rev. Astron. Ap.*, **1**, 291
Wild, J. P., Tlamicha, A. 1965, *B.A.C.*, **16**, 73
Wilson, O. C. 1966, *Science*, **151**, 1487
Wlerick, G., Axtell, J. 1957, *Ap. J.*, **126**, 253
Wolfe, J. H., Silva, R. W., McKibbin, D. D., Mason, R. H. 1966, *J. Geophys. Res.*, **71**, 3329
Wyndham, J. E. 1966, in *The Solar Wind*, 109–22 (Jet Propulsion Lab. and California Inst. Technol., Pasadena)
Zhelezniakov, V. V. 1962, *Astron. Zh.*, **39**, 5–14
Zirin, H. 1966, *The Solar Atmosphere* (Blaisdell, Waltham, Mass.)
Zirin, H., Severny, A. B. 1961, *Observatory*, **81**, 155

CONTENTS